© 2024. Published by The Company of Biologists Ltd | Development (2024) 151, dev202879. doi:10.1242/dev.202879

RESEARCH ARTICLE

Lrig1 regulates cell fate specification of glutamatergic neurons via FGF-driven Jak2/Stat3 signaling in cortical progenitors

Ana Paula De Vincenti[1,*], Antonela Bonafina[1,2,*], Fernanda Ledda[2] and Gustavo Paratcha[1,‡]

ABSTRACT

The cell-intrinsic mechanisms underlying the decision of a stem/progenitor cell to either proliferate or differentiate remain incompletely understood. Here, we identify the transmembrane protein Lrig1 as a physiological homeostatic regulator of FGF2-driven proliferation and self-renewal of neural progenitors at early-to-mid embryonic stages of cortical development. We show that Lrig1 is expressed in cortical progenitors (CPs), and its ablation caused expansion and increased proliferation of radial/apical progenitors and of neurogenic transit-amplifying $Tbr2^+$ intermediate progenitors. Notably, our findings identify a previously unreported EGF-independent mechanism through which Lrig1 negatively regulates neural progenitor proliferation by modulating the FGF2-induced IL6/Jak2/Stat3 pathway, a molecular cascade that plays a pivotal role in the generation and maintenance of CPs. Consistently, *Lrig1* knockout mice showed a significant increase in the density of pyramidal glutamatergic neurons placed in superficial layers 2 and 3 of the postnatal neocortex. Together, these results support a model in which Lrig1 regulates cortical neurogenesis by influencing the cycling activity of a set of progenitors that are temporally specified to produce upper layer glutamatergic neurons.

KEY WORDS: Lrig1, IL6/Jak2/Stat3 pathway, Cortical progenitors, Embryonic cortical development, Glutamatergic neurogenesis

INTRODUCTION

Proper development of the cerebral cortex requires a strict control and adequate coordination among the processes of cell proliferation, survival, migration and differentiation. Alterations in the number, location and subtypes of neurons generated affect functional properties of the neocortex, and could cause neurological diseases and neurodevelopmental disorders, such as schizophrenia, autism and depression (Dwyer et al., 2016). In the neocortex, the vast majority of neurons are glutamatergic and they are arranged in six horizontally oriented layers. Although not completely homogeneous, neurons located in the same layer share characteristics that include similar patterns of gene expression, morphology and connectivity (Dehay and Kennedy, 2007). The construction of this highly organized laminar circuit involves a complex sequence of events in which cortical progenitors (CPs) proliferate and differentiate phenotypically to give rise to the generation of neurons, which in turn migrate radially to their final position in the cortical circuit (Dehay and Kennedy, 2007). This process occurs in an inside-out manner, where early born neurons populate deep layers, and late-born neurons invade upper layers of the cortex (Molyneaux et al., 2007). Previous studies indicate that cortical neurogenesis requires the coordinated interaction between extracellular signals (e.g. trophic factors and mitogenic signals) and intrinsic factors (e.g. transcriptional factors and endogenous regulators of the trophic signals), which function in a cell-intrinsic and context-dependent manner (Bonnefont and Vanderhaeghen, 2021; Borrell and Reillo, 2012; Gaspard et al., 2008; Kam et al., 2014; Toma and Hanashima, 2015). Although many extracellular factors have been identified as regulators of this process, understanding the intrinsic mechanisms underlying the decision of a progenitor cell to proliferate or to generate the neurogenic progeny of a specific cortical layer still requires further investigation.

Lrig transmembrane proteins (leucine-repeat and immunoglobulin Ig-like domain proteins), constitute a family of three proteins, Lrig1, Lrig2 and Lrig3, that are enriched in the nervous system (Chen et al., 2021). Lrig1, the most studied member of this family, has been functionally characterized as an endogenous regulator of the activity of various growth factor and neurotrophic factor receptors (Alsina et al., 2016; Gur et al., 2004; Hedman and Henriksson, 2007; Laederich et al., 2004; Ledda et al., 2008; Ledda and Paratcha, 2016; Shattuck et al., 2007; Wang et al., 2013), and as a tumor suppressor, the deletion of which leads to proliferative phenotypes in the intestine, skin and cornea (Neirinckx et al., 2017; Simion et al., 2014). Furthermore, Lrig1 has been identified as an epidermal stem-cell marker, the function of which is to maintain tissue homeostasis (Jensen et al., 2009). The loss of Lrig1 promotes the proliferation of epidermal and intestinal stem cells, thus suggesting that Lrig1 might contribute to maintain the quiescence state of these cells (Jensen and Watt, 2006; Wong et al., 2012). Although it is generally assumed that the mechanism through which Lrig1 regulates stem cell quiescence is by antagonizing epidermal growth factor receptor (EGFR) activation (Ji et al., 2022), it has also recently been hypothesized that Lrig1 could regulate stem cell quiescence by promoting BMP signaling (Herdenberg and Hedman, 2023). Despite all this evidence, little is known about the biological contribution of Lrig1 during embryonic brain development.

Recently, it has been demonstrated that Lrig1 functions as a marker of long-term neurogenic stem cells in the lateral ventricles of the adult mouse brain (Nam and Capecchi, 2020). Further evidence showed that Lrig1 acts as an important regulator of neural stem cell (NSC) exit from postnatal development to adulthood in the ventricular-subventricular zone (V-SVZ) niche, limiting their persistent hyperproliferation (Marques-Torrejon et al., 2021; Nam and Capecchi, 2023). In line with this, Jeong et al. showed that, at late embryonic and perinatal stages of cortical development, Lrig1 slows the proliferation of radial progenitors as they transit to give rise

[1]Laboratorio de Neurociencia Molecular y Celular, Instituto de Biología Celular y Neurociencias (IBCN)-CONICET-UBA, Facultad de Medicina. Universidad de Buenos Aires (UBA), Buenos Aires CP1121, Argentina. [2]Fundación Instituto Leloir, Instituto de Investigaciones Bioquímicas de Buenos Aires, Buenos Aires C1405 BWE, Argentina.
*These authors contributed equally to this work

‡Author for correspondence (gparatcha@fmed.uba.ar)

A.P.D.V., 0000-0003-2051-1169; A.B., 0000-0002-6694-8449; F.L., 0000-0002-9769-6926; G.P., 0000-0002-0804-4433

Handling Editor: Debra Silver
Received 15 March 2024; Accepted 7 August 2024

Development (2024) 151, dev202879. doi:10.1242/dev.202879

to a group of postnatal NSCs. The authors show that Lrig1 mediates these effects by negatively regulating EGFR signaling (Jeong et al., 2020).

Intriguingly, Lrig1 has also been reported to be expressed earlier at the ventricular zone (VZ) of the developing cortex (Di Bella et al., 2021; Jeong et al., 2020; Telley et al., 2016; van Erp et al., 2015), at stages in which VZ cortical progenitors still did not acquire the competence to divide in response to EGF (Burrows et al., 1997; Fox and Kornblum, 2005; Fu et al., 2021; Kilpatrick and Bartlett, 1995; Kornblum et al., 1997; Lillien and Raphael, 2000). Thus, based on this evidence, we decided to further explore the contribution of Lrig1 from early-to-mid embryonic stages of cortical proliferation, as well as its consequences for the postnatal differentiation of layer-specific glutamatergic cortical neurons.

Here, we show that Lrig1 is expressed at early-to-mid stages of cortical development in neural stem and progenitor cells. Moreover, we show that *Lrig1* deficiency promotes the expansion and proliferation of radial and apical progenitors, which results in an increase of Tbr2-positive intermediate progenitors. Our results indicate that Lrig1 mediates these effects by modulating the FGF2 response via interleukin 6 (IL6)/Janus kinase 2 (Jak2)/Stat3 activation on CPs. The long-lasting effects of *Lrig1* deficiency involve a promotion of the production of upper layer glutamatergic neurons, thereby modulating cortical morphogenesis. Together, our results reveal that Lrig1 functions as a homeostatic regulator of glutamatergic cortical development.

RESULTS

Lrig1 is highly expressed during early and middle embryonic cortical development

To explore whether Lrig1 could be involved in the control of embryonic cortical development, we analyzed its mRNA expression by semi-quantitative and real-time RT-PCR. The highest expression of *Lrig1* mRNA was detected on embryonic days (E) 12 and E14, when the neocortex is composed primarily of actively dividing neural progenitors, and neurogenesis is ongoing. Lrig1 was still present in the rat cortex at E16 and its expression dropped markedly after this stage (Fig. 1A). The expression pattern of *Fgfr1* mRNA, which mediates the mitogenic effect of fibroblast growth factor (FGF) in early precursor cells, follows the same expression pattern of Lrig1 during embryonic development of the neocortex (Fig. 1A,B). Consistent with a previous report showing that Lrig1 slows EGF-induced proliferation of radial progenitors at perinatal stages of cortical development (Jeong et al., 2020), we observed prominent expression of *Egfr* mRNA around birth (Fig. 1A). An expanded analysis of *Lrig1* mRNA expression in rat neocortex, including E18,

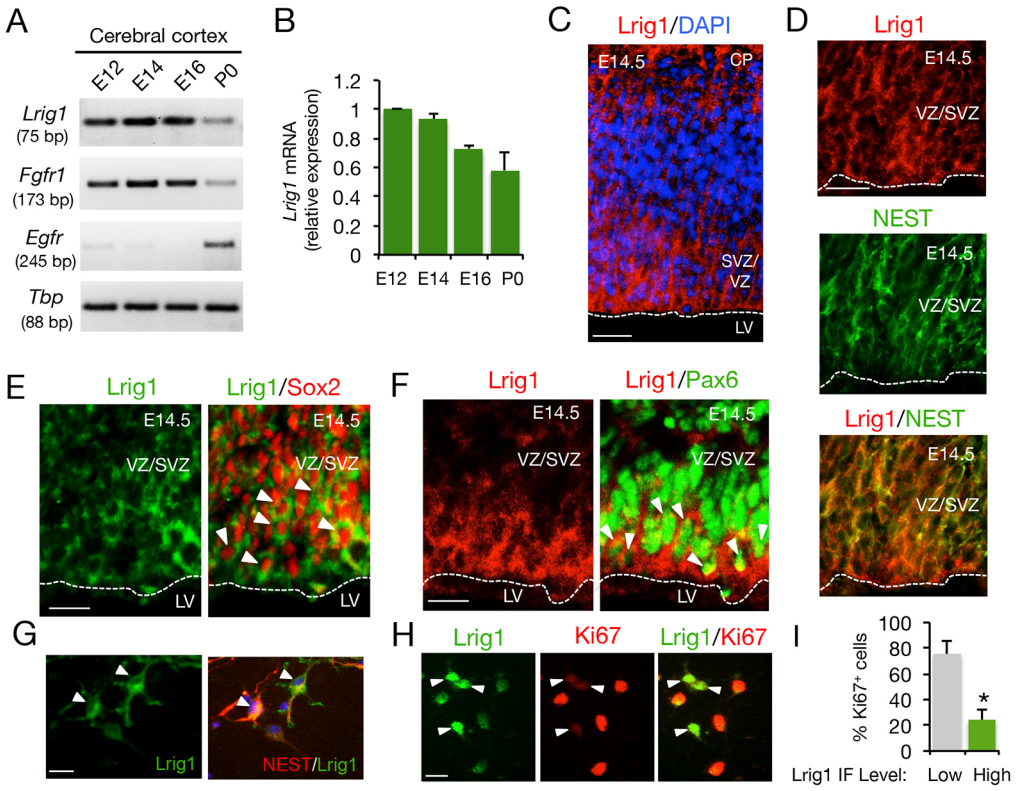

Fig. 1. Developmental expression and localization of Lrig1 during cortical development. (A) Analysis of developmental expression of *Lrig1*, *Fgfr1* and *Egfr* mRNA by semi-quantitative RT-PCR in rat cortex at the indicated embryonic days (E) and in newborn (P0). (B) Quantitative analysis of developmental expression of *Lrig1* mRNA by real-time qPCR. Data are mean±s.e.m. of n=3 independent samples. *Lrig1* mRNA levels were normalized to the expression of the housekeeping gene *Tbp* (TATA box-binding protein). (C) Localization by immunofluorescence of Lrig1 in coronal sections of rat E14.5 cortex. CP indicates the cortical plate. Scale bar: 25 µm. (D-F) Co-expression of Lrig1 (red) and nestin (NEST, green) (D), Lrig1 (green) and the neural progenitor marker Sox2 (red) (E), and Lrig1 (red) and the radial progenitor marker Pax6 (green) (F) is shown in coronal sections of rat E14.5 cortex. LV, lateral ventricle; VZ, ventricular zone; SVZ, subventricular zone. Arrowheads indicate co-expression. Scale bars: 20 µm. (G) Co-expression of Lrig1 (green) and the neural-stem cell marker nestin (NEST, red) in dissociated primary cortical progenitors. Scale bar: 25 µm. (H) Dissociated cortical progenitor cells immunostained for Lrig1 (green) and the proliferative marker Ki67 (red). Arrowheads indicate non-proliferating (Ki67$^-$) cells expressing high levels of Lrig1. Scale bar: 25 µm. (I) Bar graph shows the percentage of Ki67$^+$ cells (red) expressing low and high levels of Lrig1 (green). High Lrig1 expression inversely correlated with cell proliferation. *P<0.05, unpaired, two-tailed Student's t-test.

Development (2024) 151, dev202879. doi:10.1242/dev.202879

when gliogenesis is taking place, showed a marked decrease of *Lrig1* at this stage followed by a modest increment at P0 (Fig. S1A).

To define the localization and cell types expressing Lrig1, we performed immunofluorescence analysis of E14.5 rat cortical sections. We found that Lrig1 expression heavily overlapped with the neural stem cell marker nestin and the neural progenitor marker Sox2, which are placed in the proliferative ventricular (VZ) and subventricular zone (SVZ) of the developing cortex. Co-expression between Lrig1 and the radial progenitor cell marker Pax6 was also detected in the VZ. Lrig1 immunoreactivity was localized in neural progenitors following a pattern consistent with plasma membrane localization (Fig. 1C-F). The expression of Lrig1 was additionally confirmed in mouse cortical sections of E12.5 and E13.5, and the antibody used against Lrig1 was further validated by immunofluorescence in sections of *Lrig1* KO mice (Fig. S1B,C). In support of our findings, a mouse transcriptomic study of scRNA-seq (Di Bella et al., 2021) also shows that *Lrig1* is expressed from early-to-mid stages (E10-E13) of embryonic development of the mouse neocortex in apical progenitors, followed by a later expression at postnatal day 1 (P1) and P4 in glial cells (Fig. S1D).

Dissociated cultures of CPs also showed expression of Lrig1 in Nestin-positive cells (Fig. 1G). Interestingly, in CP primary cultures, cells expressing high levels of Lrig1 were not proliferative (negative for the proliferative marker Ki67), whereas cells expressing low levels of Lrig1 were actively cycling (Ki67-positive cells). Thus, this result revealed that the expression of Lrig1 inversely correlated with cell proliferation, suggesting that Lrig1 could be maintaining neural stem and progenitor cells in a resting state (Fig. 1H,I).

Lrig1 ablation promotes proliferation and self-renewal of embryonic cortical progenitors in response to FGF

Based on our observation, indicating that Lrig1 expression inversely correlates with Ki67 expression (Fig. 1H,I), we decided to analyze whether Lrig1 could be involved in the control of CP cell proliferation. To this end, we performed a neurosphere assay from cortices of wild-type and *Lrig1*-deficient mice at embryonic day (E) 13.5. This assay is a useful technique to evaluate the proliferative capacity of a cell population, as only highly proliferative progenitors have the ability to form spheres and grow in suspension in the presence of mitogenic factors, such as FGF2 and EGF. In this culture condition, we found that *Lrig1* deficiency promotes a significant increase in the number of neurospheres formed from E13.5 CPs treated with FGF2 or with FGF2 and EGF, but not from progenitors cultured with EGF alone (Fig. 2A) (Burrows et al., 1997), indicating that, at this embryonic stage, Lrig1 dampens proliferation of CPs induced by FGF. In addition, our data showed that Lrig1 deficiency increases not only the number but also the diameter of the neurospheres formed by FGF (Fig. 2B,C).

We also evaluated by immunofluorescence the proportion of Ki67-positive cells and the percentage of proliferating precursors (Ki67 and nestin double-positive cells) in individual spheres grown in the presence of FGF2. We observed that neurospheres obtained from *Lrig1*-deficient mice showed an increased proportion of Ki67-expressing cells and also a higher rate of proliferating precursors (Fig. 2D-F). Neurospheres have cells at different stages of neuronal differentiation, and only a small fraction of them maintain the initial proliferative capacity to re-form spheres, thus giving rise to secondary spheres (Reynolds and Weiss, 1996). When secondary neurospheres were obtained from the primary neurospheres, we observed that the absence of Lrig1 still generated more spheres than control spheres. This result indicates that *Lrig1* deficiency favors the expansion of the population of progenitors with proliferative capacity to generate new secondary neurospheres (Fig. 2G-I). Thus, the loss of *Lrig1* confers not only greater proliferation but also a higher capacity for self-renewal.

To explore whether *Lrig1* deficiency could affect the cell division mode of neural stem/progenitor cells, we performed a paired cell assay (Ahmad et al., 2019). Wild-type and *Lrig1*-deficient progenitor cells were seeded at low density in adherent culture conditions for 20 h with FGF2, and then fixed and stained with Ki67 and DAPI. Cell pairs were scored as having symmetric proliferative division when both daughter cells were $Ki67^+$, pairs were scored as having asymmetric division when one daughter cell was $Ki67^+$ and the other one was $Ki67^-$, and pairs were scored as having symmetric terminal division when both daughter cells were negative for Ki67. *Lrig1* knockout cells had a higher frequency of symmetric proliferative divisions and a lower proportion of symmetric terminal divisions compared with controls (Fig. 2J,K). Thus, in the presence of FGF2, *Lrig1* ablation increases the proportion of cycling and self-renewing progenitor cells.

Lrig1 overexpression inhibits FGF2-induced proliferation of embryonic cortical progenitors

We then performed gain-of-function assays by transducing neural precursor cell cultures with a retroviral vector expressing Lrig1. We used either retrovirus control (RV-Control) or retrovirus overexpressing Flag-Lrig1 (RV-Flag-Lrig1) in neurosphere cultures grown in the presence of FGF2. In this culture system, we found that Lrig1 overexpression significantly inhibited the number and diameter of FGF2-induced neurospheres (Fig. 3A-D). We also evaluated by immunofluorescence the proportion of Ki67-positive cells and the percentage of proliferating precursors (Ki67 and nestin double-positive cells) in individual spheres. We observed that neurospheres infected with RV-Flag-Lrig1 showed lower proportion of Ki67-positive cells and a decreased rate of Nestin-positive proliferating precursors (Fig. 3E-G). Thus, all these culture assays demonstrated that Lrig1 is a regulator of CP cell proliferation, maintaining cells in a resting state.

Lrig1 regulates cell cycle progression by modulating the expression levels of cyclin D1, Myc and cyclin-dependent kinase inhibitor p27 in response to FGF2

Neurospheres grown in the presence of FGF2 are characterized by upregulation of cell cycle promoters such as cyclins and Myc proto-oncogene, as well as by a decrease in the expression levels of cell cycle inhibitors (Lukaszewicz et al., 2002; Mira et al., 2010). At this point, we analyzed by semi-quantitative RT-PCR the expression levels of cell-cycle regulatory genes such as *Ccnd1* (cyclin D1), *Ccne1* (cyclin E), *Myc* and cyclin-dependent kinase inhibitor p27 (*Cdkn1b*), in neurospheres derived from wild-type and *Lrig1*-deficient mice. From these experiments, we observed that, in neurospheres derived from *Lrig1* mutants, the mRNA expression of *Ccnd1* and *Myc* increased significantly compared with the levels detected in wild-type neurospheres grown in the presence of FGF2. In addition, we observed that neurospheres derived from *Lrig1 KO* mice also showed a significant downregulation of the levels of cyclin-dependent kinase inhibitor *Cdkn1b* mRNA (Fig. 4A,B). Thus, this finding indicates that *Lrig1* deficiency regulates the cycling activity of neural precursors by controlling the expression levels of positive and negative regulators of cell cycle progression in response to FGF2.

To understand how Lrig1 could affect the cell cycle, we performed proliferation and cell cycle exit assays. To this end, dissociated CPs from control and *Lrig1*-deficient mice were cultured in the presence of FGF2 for 5 DIV. After this, the cells were pulse labeled with BrdU

Development (2024) 151, dev202879. doi:10.1242/dev.202879

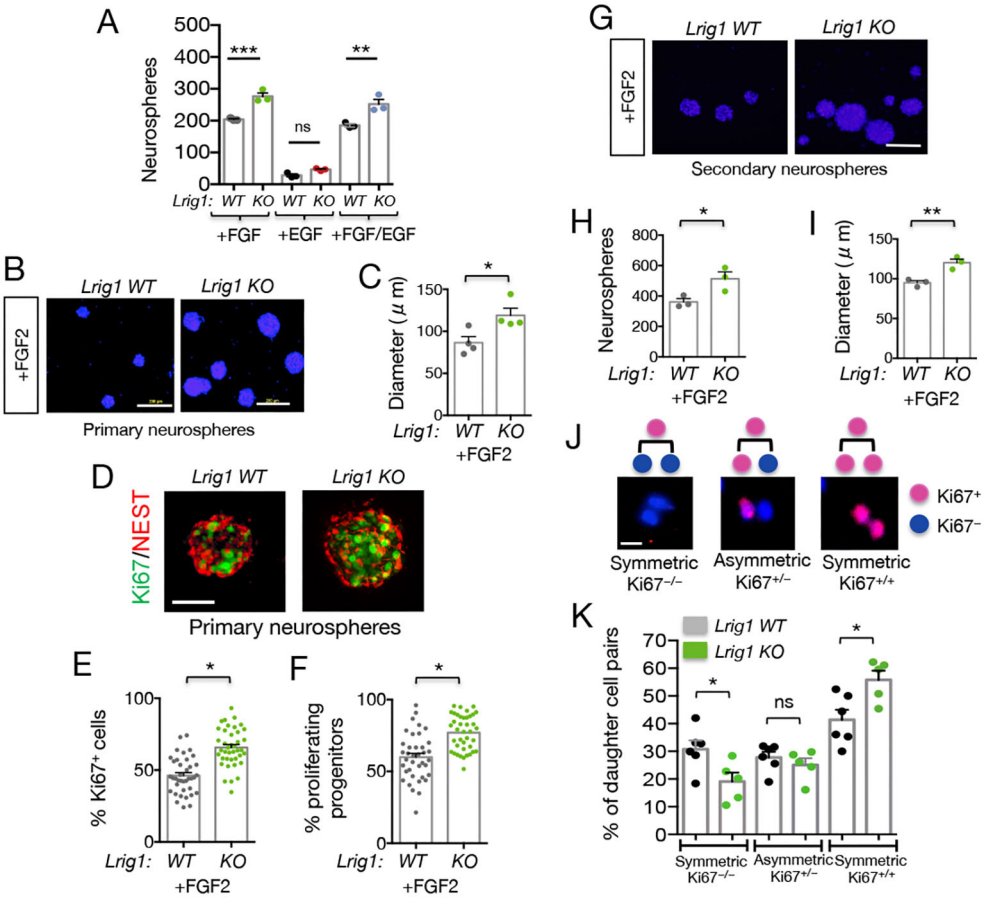

Fig. 2. *Lrig1* deficiency increases proliferation and self-renewal of embryonic cortical progenitor cells in response to FGF2. (A) Bar graph shows the quantification of the number of neurospheres obtained from *Lrig1* wild-type and *Lrig1* KO progenitor cells grown in the presence of FGF2 (10 ng/ml), EGF (10 ng/ml), or FGF2 and EGF (10 ng/ml of each). Data are mean±s.e.m., n=3 independent assays. ***P<0.005, **P<0.01 by ANOVA followed by Tukey's multiple comparison test. (B) Representative images of neurospheres from control and *Lrig1*-deficient cortical precursor cells grown for 5 DIV in the presence of FGF2 (10 ng/ml) and stained with DAPI. Scale bars: 200 µm. (C) Bar graphs show the quantification of the diameter of neurospheres from *Lrig1* wild-type and *Lrig1* KO progenitor cells grown in the presence of FGF2 (10 ng/ml). Data are mean±s.e.m., n=4 independent assays. *P<0.05, unpaired, two-tailed Student's t-test. (D) Images of neurospheres derived from *Lrig1* wild-type and *Lrig1*-deficient cortical precursor cells grown as described in A stained for nestin (NEST, in red) and Ki67 (green). Scale bar: 50 µm. (E,F) Bar graphs show the quantification of the percentage of Ki67$^+$ cells (Ki67$^+$/DAPI) and the percentage of proliferating precursors (Ki67$^+$nestin$^+$/nestin$^+$) per sphere grown in the presence of FGF2 (10 ng/ml). Data are mean±s.e.m., n=3 independent assays (dots represent 40 neurospheres/experimental group). *P<0.05, unpaired, two-tailed Student's t-test. (G) Representative images of secondary DAPI-stained neurospheres generated from cortical precursor cells dissociated from primary spheres. Scale bar: 200 µm. (H,I) Bar graphs show the quantification of the number and diameter of secondary neurospheres from *Lrig1* wild-type and *Lrig1* KO progenitor cells grown in the presence of FGF2. Data are mean ±s.e.m., n=3 independent assays. *P<0.05, **P<0.01, unpaired, two-tailed Student's t-test. (J) Paired cell assay showing representative images of Ki67 immunostaining. Scale bar: 5 µm. (K) Bar graph showing the percentage of symmetric proliferative, asymmetric and symmetric terminal divisions of *Lrig1* wild-type and *Lrig1*-deficient cortical progenitors cultured at low density in the presence of FGF2 (25 ng/ml) for 20 h. Data are mean±s.e.m., n=6 *Lrig1* wild-type and n=5 *Lrig1* KO independent cultures. ns, not significant, *P<0.05, unpaired, two-tailed Student's t-test.

for 4 h and maintained additionally for 24 h before fixation. The fraction of CP cells that left the cell cycle was identified as BrdU$^+$ and Ki67$^-$. As shown in Fig. 4C, dissociated CPs coming from *Lrig1*-deficient mice show a significant increase in cell proliferation while showing a significant reduction in the proportion of cells exiting the cell cycle when compared with wild-type cells. Thus, altogether our findings indicate that *Lrig1* deficiency increases proliferation by promoting the continued cycling of embryonic cortical progenitors rather than their exit from the cell cycle and differentiation.

Lrig1 regulates FGF2-induced Jak2/Stat3 signaling in neocortical progenitors

Based on previous evidence showing that Lrig1 regulates different receptor tyrosine kinases (RTKs) and that Lrig3 interacts with FGFR1 (Zhao et al., 2008), we examined whether Lrig1 could co-immunoprecipitate with this receptor in lysates prepared from embryonic cortices. Intriguingly, we were not able to detect association between Lrig1 and FGFR1 *in vivo* (Fig. S2).

To obtain additional insight into the mechanism through which Lrig1 controls FGF-induced CP cell proliferation, we decided to evaluate the contribution of the Jak2/Stat3 pathway, which is present in neural progenitors of the mouse embryonic neocortex, and plays an essential role in the generation and maintenance of radial glia progenitors (Hong and Song, 2015). Indeed, the Jak2/Stat3 signaling cascade is part of a network of pathways activated by FGF2 that is required for proliferation of progenitor cells (Todd et al., 2016) and for formation of FGF2-dependent neurospheres (Yoshimatsu et al., 2006). Furthermore, a negative regulation of the Stat3 pathway by Lrig1 has been demonstrated in corneal epithelial stem cells (Nakamura et al.,

Development (2024) 151, dev202879. doi:10.1242/dev.202879

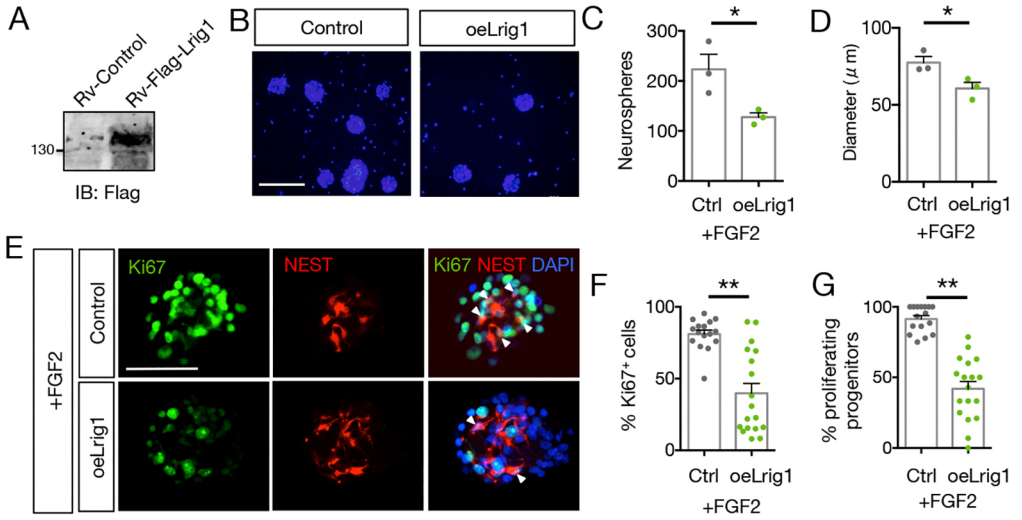

Fig. 3. *Lrig1* overexpression restricts FGF-induced proliferation of embryonic cortical progenitor cells. (A) Representative Flag immunoblot showing exogenous expression of Flag-tagged Lrig1 in HEK-293 cells transduced with either control or Flag-Lrig1 retrovirus. (B) Representative images of control and Lrig1-overexpressing (oeLrig1) neurospheres grown for 7 DIV in the presence of FGF2 (15 ng/ml) and stained with DAPI. Scale bar: 200 µm. (C,D) Bar graphs show the quantification of the number and diameter of neurospheres transduced with either control or retroviral vector overexpressing Lrig1. Data are mean±s.e.m., n=3 independent assays. *P<0.05, two-tailed Student's t-test. (E) Images of neurospheres derived from control and *Lrig1*-overexpressing cortical precursor cells grown as described in B and stained for nestin (red) and Ki67 (green), and with DAPI. Arrowheads show proliferating Ki67$^+$ nestin$^+$ progenitor cells. Scale bar: 50 µm. (F,G) Bar graphs show the quantification of the percentage of Ki67$^+$ cells (Ki67$^+$/DAPI) and the percentage of proliferating precursors (Ki67$^+$ nestin$^+$/nestin$^+$) per sphere grown in the presence of FGF2 (15 ng/ml). Data are mean±s.e.m. Individual values represent determinations of n=16 (Ctrl) and n=18 (oeLrig1) neurospheres from three independent assays. **P<0.01, two-tailed Student's t-test.

2014). Therefore, all this evidence led us to evaluate whether Lrig1 might be regulating the FGF2-induced Jak2/Stat3 pathway in E13.5 cortical progenitors. After exploring the co-expression of Lrig1 and Stat3 in embryonic cortical apical progenitors (Fig. S3), we examined the capacity of Lrig1 to regulate FGF2-induced Jak2-mediated cell proliferation in wild-type and *Lrig1* knockout neurospheres grown for 5 days in the presence of FGF2 and then treated, or not, with the Jak2 kinase inhibitor AG490 (20 µM) for an additional 24 h. We evaluated by immunofluorescence the relative proportion of proliferating Ki67$^+$ cells (Ki67$^+$/DAPI) and the percentage of Ki67$^+$ neural progenitor

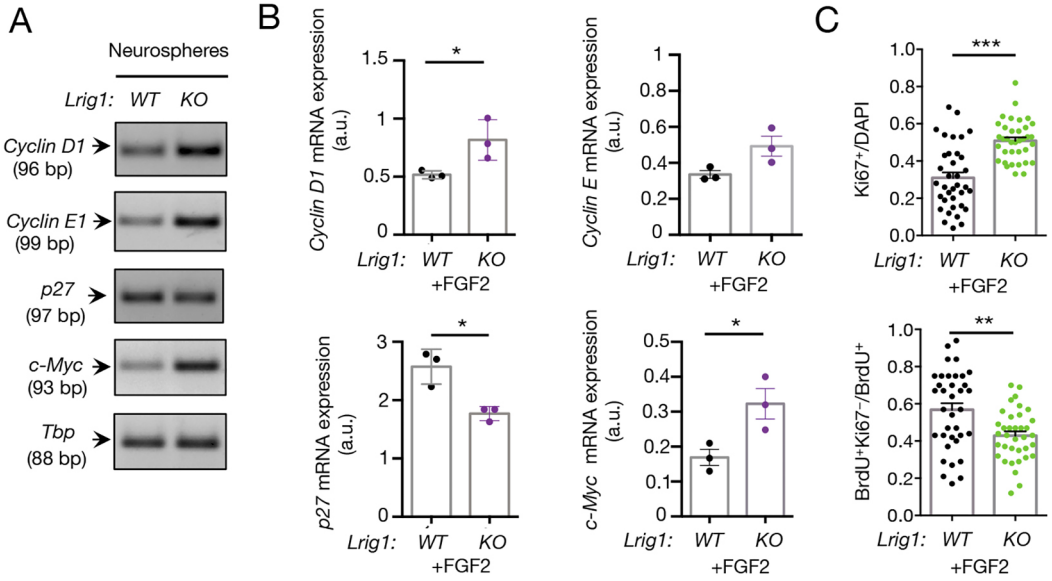

Fig. 4. Lrig1 controls cell cycle progression by modulating the expression of cell-cycle regulators in response to FGF2. (A) Semi-quantitative RT-PCR analysis of *Ccnd1* (cyclin D1), *Ccne1* (cyclin E), *Tbp*, *Myc* and cyclin-dependent kinase inhibitor p27 (*Cdkn1b*) mRNA expression from *Lrig1* wild-type and *Lrig1* KO neurospheres cultured in the presence of 10 ng/ml of FGF2. For each molecule, the PCR amplification product size is indicated in base pairs (bp). (B) Bar graphs showing the levels of cyclin D1, cyclin E, *p27* and *Myc* mRNA levels expressed as arbitrary units (a.u.). The mRNA levels were normalized to the expression of the housekeeping gene *Tbp*. Data are mean±s.e.m. from n=3 independent cultures. *P<0.05, two-tailed Student's t-test. (C) Bar graphs show the quantification of the proportion of *Lrig1* wild-type and *Lrig1* KO cortical progenitor cells that are Ki67$^+$ (Ki67$^+$/DAPI) (upper graph) and (BrdU$^+$ Ki67$^-$/BrdU$^+$) (lower graph) cultured in the presence of FGF2 (10 ng/ml). Data are mean±s.e.m. Individual values represent determinations of n=36 (wild type) and n=36 (KO) fields from three independent assays. **P<0.01, ***P<0.001, two-tailed Student's t-test.

Development (2024) 151, dev202879. doi:10.1242/dev.202879

cells (Ki67$^+$Nestin$^+$/Nestin$^+$) in individual spheres. Interestingly, we observed that although *Lrig1*-deficient neurospheres showed a significant increase in both the proportion of Ki67$^+$ cells and the percentage of proliferating progenitor cells, the treatment with AG490 blocked both effects, indicating that Lrig1 regulates CP cell proliferation by inhibiting FGF2-driven Jak2 activation (Fig. 5A-C). Additionally, we ensured that AG490 effectively blocked Jak2/Stat3 activation in our culture conditions (Fig. S4A,B).

This finding led us to evaluate whether Lrig1 might be regulating Stat3 phosphorylation in Tyr^{705}, an event that correlates with its activation by Jak2. For this purpose, we grew either control or Lrig1-overexpressing neurospheres by using retroviral vectors, and then evaluated by immunofluorescence the relative proportion of pStat3$^+$ cells (pStat3$^+$/DAPI) and the percentage of pStat3$^+$ neural progenitor cells (pStat3$^+$ nestin$^+$/nestin$^+$) in individual spheres. We observed that neurospheres overexpressing Lrig1 (oeLrig1) showed a significant reduction in both the proportion of Stat3 activated cells and the percentage of neural progenitor cells (NPCs) expressing Stat3 phosphorylated on Tyr^{705} (Fig. 5D-F), indicating that Lrig1 could inhibit FGF2-mediated neurosphere formation by

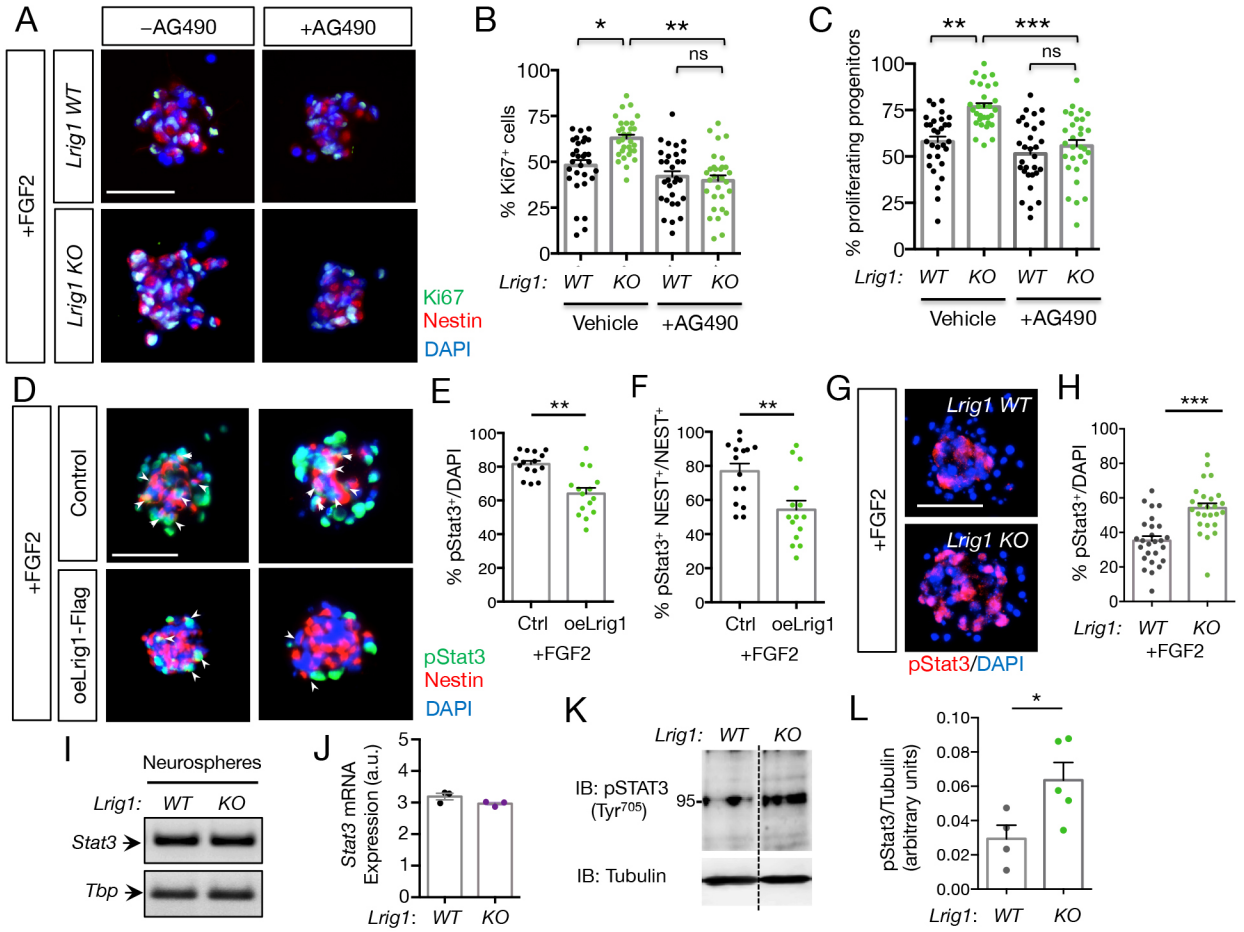

Fig. 5. Lrig1 inhibits FGF-induced Jak2/Stat3 signaling in neocortical progenitors. (A) Representative images of *Lrig1* wild-type and *Lrig1* KO neurospheres grown for 5 DIV in the presence of FGF2 (10 ng/ml) and then treated with vehicle (DMSO, –AG490) or AG490 (20 µM) for additional 24 h. Cell proliferation was evaluated in neurospheres stained using the antibodies anti-Ki67 (green) and anti-nestin (red), and with DAPI (blue). Scale bar: 50 µm. (B,C) Bar graphs show the quantification of (B) the percentage of Ki67$^+$ cells (Ki67$^+$/DAPI) and (C) the percentage of Ki67$^+$ progenitor cells (Ki67$^+$ nestin$^+$/nestin$^+$) in wild-type and *Lrig1*-deficient neurospheres cultured as described in A. Data are mean±s.e.m., *n*=30 neurospheres per condition were analyzed from three mice of each genotype. **P*<0.05, ***P*<0.01 and ****P*<0.005, two-tailed Student's *t*-test. ns, not significant. (D) Representative images of control and Lrig1-overexpressing (oeLrig1) neurospheres grown for 7 DIV in the presence of FGF2 (15 ng/ml) and stained using the antibodies anti-pStat3 (Tyr 705) (green) and anti-nestin (red), and with DAPI (blue). Arrowheads indicate pStat3/nestin double-positive cells. Scale bar: 50 µm. (E,F) Bar graphs show (E) the quantification of the percentage of pStat3$^+$ cells (pStat3$^+$/DAPI) and (F) the percentage of pStat3$^+$ progenitor cells (pStat3$^+$ nestin$^+$/nestin$^+$) in neurospheres transduced with either control or retroviral vector overexpressing Lrig1. Data are mean±s.e.m., *n*=15 neurospheres from three independent assays were analyzed per condition. ***P*<0.01, two-tailed Student's *t*-test. (G) Representative images of *Lrig1* wild-type and *Lrig1* KO neurospheres grown for 5 DIV in the presence of FGF2 (10 ng/ml) and stained using anti-pStat3 (Tyr 705) (red) and DAPI (blue). Scale bar: 50 µm. (H) Bar graph shows the quantification of the percentage of pStat3$^+$ cells (pStat3$^+$/DAPI) in *Lrig1* wild-type and *Lrig1* KO neurospheres treated with FGF2. Data are mean±s.e.m., *n*=26 neurospheres from three independent assays were analyzed per condition. ***P*<0.001, two-tailed Student's *t*-test. (I) Semi-quantitative RT-PCR analysis of *Stat3* mRNA expression from wild-type and *Lrig1KO* neurospheres cultured in the presence of 10 ng/ml of FGF2. PCR amplification product size is indicated in base pairs (bp). (J) Bar graph shows the levels of *Stat3* mRNA expressed as arbitrary units (a.u.). The mRNA levels were normalized to the expression of the housekeeping gene *Tbp*. Data are mean±s.e.m. from *n*=3 independent cultures. (K) Representative immunoblot of Stat3 phosphorylated on Tyr^{705} (pStat3) in cortical extracts from E13.5 *Lrig1* wild-type and *Lrig1* KO mice. Dotted line indicates representative bands cut from the same immunoblot image. (L) Bar graph shows the quantification of Stat3 phosphorylation (pStat3) in cortical lysates isolated from E13.5 *Lrig1* wild-type and *Lrig1* KO mice. Stat3 phosphorylation was normalized to the signal intensity of tubulin and expressed as arbitrary units (a.u.). Data are mean±s.e.m. from *n*=4 *Lrig1* wild-type and *n*=5 *Lrig1* KO mice. **P*<0.05, two-tailed Student's *t*-test.

Development (2024) 151, dev202879. doi:10.1242/dev.202879

restricting the activation of the Jak2/Stat3 signaling pathway. Interestingly, we detected a fraction of pStat3^{+}/nestin^{-} cells that might represent Tbr2^{+} intermediate progenitor cells, most of which have been reported to lack nestin expression (Englund et al., 2005). Retrovirus-mediated expression of Lrig1 in primary neurospheres was controlled by immunoblotting (Fig. S5). Likewise, neurospheres derived from *Lrig1*-deficient mice showed a significant increase in the proportion of pStat3^{+} cells (Fig. 5G,H). Analysis of *Stat3* mRNA expression levels in wild-type and *Lrig1* KO neurospheres did not show differences (Fig. 5I,J), indicating that Lrig1 regulates the activation of Stat3 without affecting the expression levels of its mRNA.

Next, we analyzed by immunoblotting the levels of phosphorylated Stat3 in cortices isolated from E13.5 wild-type and *Lrig1* KO mice. This assay revealed that *Lrig1* deficiency promotes a significant increase in Stat3 Tyr^{705} phosphorylation in the neocortex *in vivo* (Fig. 5K,L). This finding implies that Lrig1 might control CP proliferation functioning as a negative regulator of the Stat3 pathway in the developing neocortex.

Lrig1 regulates IL6 signaling in embryonic cortical progenitors

Based on previous studies showing that IL6 has proliferative effects on E12.5 cortical progenitors (Gallagher et al., 2013), and that FGF2 induces IL6 secretion (Andoh et al., 2004; Kozawa et al., 1997) and gp130 receptor expression (Todd et al., 2016) in different cellular contexts, we decided to analyze the role of this cytokine in *Lrig1* wild-type and *Lrig1* KO cortical progenitors.

Analysis of the expression of *Il6* and its receptors, *Gp130* (*Il6st*) and *Il6ra*, by RT-PCR in FGF2-induced neurospheres showed that they are expressed in our experimental system (Fig. 6A). Moreover, we observed that both IL6 receptor mRNAs are significantly induced upon FGF2 treatment of dissociated cortical progenitors, evidencing a mechanistic link between FGF2 and IL6 signaling in these cells (Fig. 6B-D). This evidence prompted us to analyze whether IL6 could be mediating the regulatory role of Lrig1 on FGF2-driven Jak2/Stat3 proliferative signaling in embryonic cortical progenitors. After confirming that IL6 receptor signaling immunoreactivity was detectable in Lrig1^{+} cortical apical precursors *in vivo* by examining *Gp130* levels (Fig. 6E), we performed neurosphere assays to evaluate whether Lrig1 could modulate Stat3 activation in neurospheres induced with IL6 alone. As it is shown in Fig. 6F,G, *Lrig1* deficiency promoted a significant increase in the proportion of pStat3^{+} (% pStat3^{+}/DAPI) cells, indicating that Lrig1 represents a negative regulator of IL6 proliferative signaling in cortical progenitors.

Lrig1 deletion enhances proliferation of embryonic cortical progenitors *in vivo*

To determine the physiological relevance of Lrig1 for cortical progenitor cell proliferation, we first evaluated the relative number of Sox2-positive radial/apical progenitors and the proportion of apical proliferating progenitors (Ki67^{+}Sox2^{+}/Sox2^{+}) by immunofluorescence staining of forebrain sections obtained from E13.5 wild-type and *Lrig1*-null mice. In agreement with our *in vitro* assays, the cortices of the *Lrig1* knockout mice showed a significant

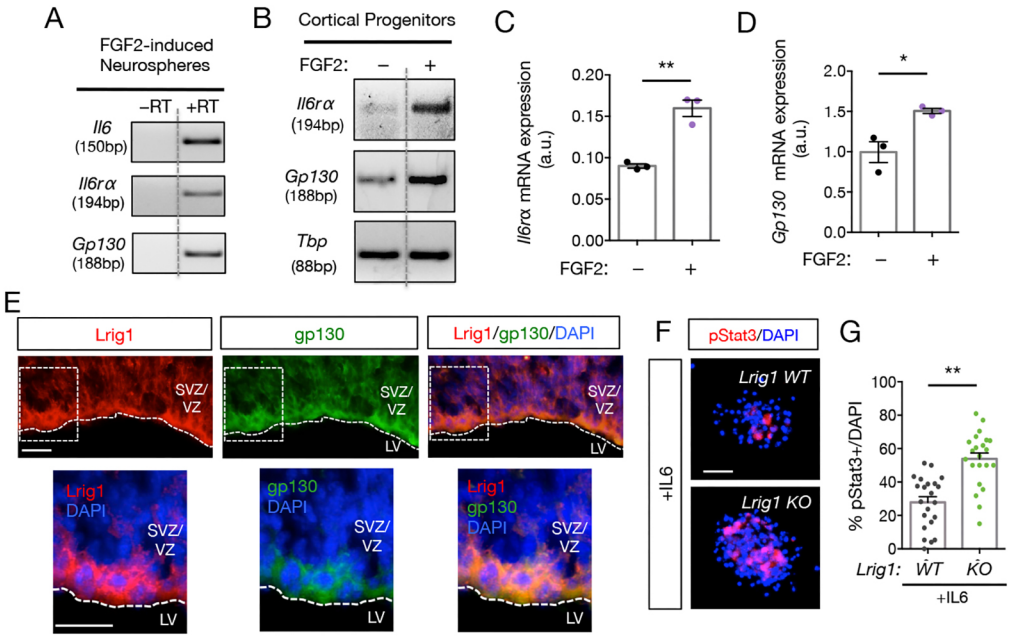

Fig. 6. Lrig1 regulates IL6 signaling in embryonic cortical progenitors. (A) Expression of *Il6*, *Il6ra* and *Gp130* mRNA by semi-quantitative RT-PCR in FGF2-induced neurospheres. Each pair of bands are from the same gel, and the dotted line indicates where lanes were removed from the gel images. (B) Expression of IL6 receptors (*Il6ra* and *Gp130* mRNA) by semi-quantitative RT-PCR in cortical progenitors treated or not with FGF2. Each pair of bands is from the same gel; the dotted line indicates where lanes were removed from the gel images. (C,D) Quantitative analysis of *Il6ra* (C) and *Gp130* (D) mRNA by semi-quantitative RT-PCR. *Il6ra* and *Gp130* mRNA levels were normalized to the expression of the housekeeping gene *Tbp* (TATA box-binding protein). Data are mean±s.e.m. of *n*=3 independent samples. **P*<0.05, ***P*<0.01, two-tailed Student's *t*-test. (E) Low-magnification (upper) and high-magnification (lower) images showing Lrig1 (red) and gp130 (green) immunostaining in the VZ and/or SVZ of rat cortex at E14.5. Scale bars: 30 µm. (F) Representative images of *Lrig1* wild-type and *Lrig1* KO neurospheres grown for 5 DIV in the presence of IL6 (100 ng/ml) and stained using anti-pStat3 (Tyr 705) (red) and DAPI (blue). Scale bar: 25 µm. (G) Bar graph shows the quantification of the percentage of pStat3^{+} cells (pStat3^{+}/DAPI) in *Lrig1* wild-type and *Lrig1* KO neurospheres treated with IL6. Data are mean±s.e.m., *n*=22 neurospheres from three independent assays were analyzed per condition. ***P*<0.01, two-tailed Student's *t*-test.

Development (2024) 151, dev202879. doi:10.1242/dev.202879

increase in both density of $Sox2^+$ radial/apical progenitors and the proportion of proliferating progenitors Sox^+Ki67^+ (Fig. 7A-C). Consistent with this, the thickness of the $Sox2^+$ proliferative domain was also significantly increased in the cortices of *Lrig1* knockout mice. The largest increase in the thickness of the $Sox2^+$ layer was detected at the most ventral level of the VZ (Fig. 7D). In contrast to what we observed for $Sox2^+$ apical progenitors, no significant difference was observed in the proportion of proliferating $Ki67^+$ $Sox2^-$ progenitor cells located in the SVZ and IZ of *Lrig1* wild-type and *Lrig1* KO cortex at E13.5 (Fig. 7E). This population of proliferating $Ki67^+$ $Sox2^-$ progenitors represents the vast majority of immunopositive $Tbr2^+$ cells, which lack expression of key transcriptional regulators of apical and/or radial glial cell (RGC) self-renewal, including Sox2 and Pax6 (Englund et al., 2005; Sessa et al., 2008). Therefore, these results suggest that Lrig1 control the proliferation of $Sox2^+$ apical progenitors but not $Sox2^-$ intermediate progenitors.

As *Lrig1* deficiency promotes the proliferation of radial and apical progenitors, we decided to explore whether *Lrig1* ablation could affect the density of intermediate progenitor, characterized by the expression of Tbr2. Comparatively, the cortices of the *Lrig1* knockout mice showed a significant increase in the total number of $Tbr2^+$ progenitors and a broader distribution in the SVZ (Fig. 7F,G). Together, these findings demonstrate that Lrig1 is a homeostatic regulator of neural precursor cell proliferation, which is able to regulate the pool size of apical and intermediate progenitors at mid-embryonic stages of cortical development.

Lrig1 ablation promotes production of upper-layer glutamatergic neuron in the postnatal neocortex

Finally, we asked how the increased levels of CPs detected in *Lrig1* knockout mice could affect glutamatergic cortical neurogenesis at postnatal stages. To assess this, we first conducted immunostaining for the neuronal marker NeuN to evaluate the proportion of neurons present in superficial and deep cortical layers of P15 wild-type and *Lrig1*-deficient mice. Results from this experiment showed a significant increase in the density of $NeuN^+$ cells in cortical layers 2 and 3, but not in cortical layers 5 and 6 of *Lrig1*-deficient mice relative to wild-type littermates (Fig. S6). To further characterize this result, we then performed layer-specific immunostainings for the early-born deep layer neuron markers Ctip2 (L5 and L6) and Tbr1 (L6), together with three later-born upper layer markers, Cux1 (L2/3), Satb2 (L2/3) and CART (L3). We analyzed their distributions in cortical sections of P15 wild-type and *Lrig1* knockout mice, when

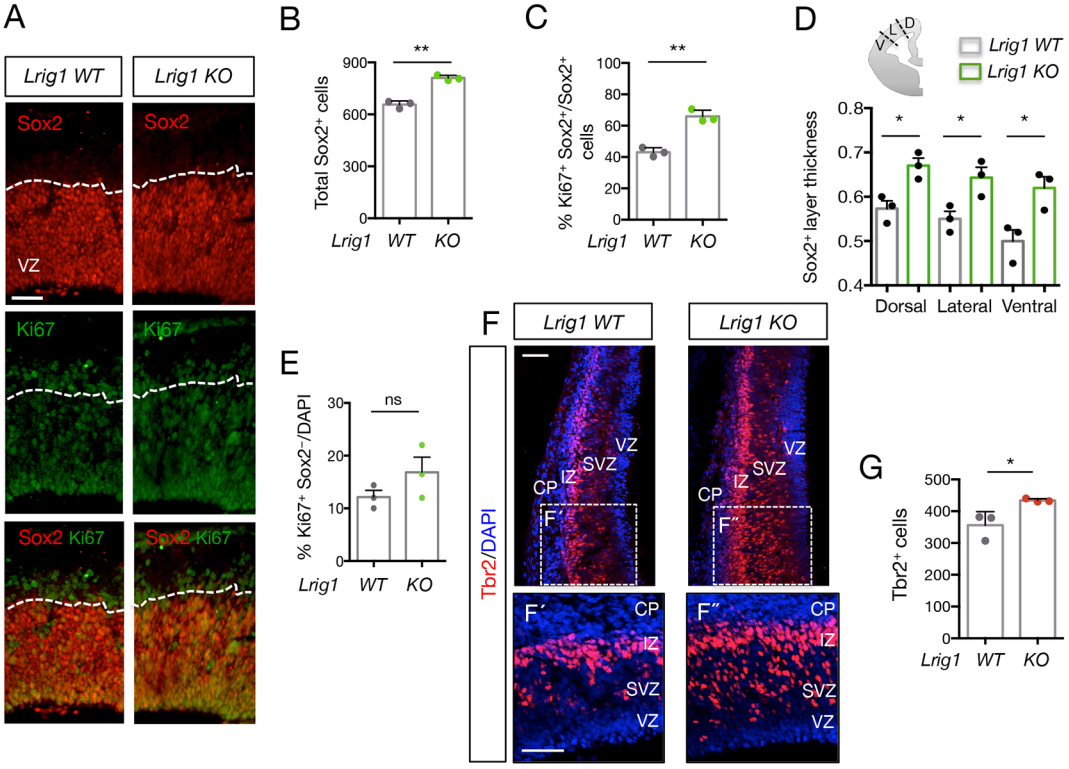

Fig. 7. *Lrig1* ablation increases proliferation of embryonic cortical progenitors *in vivo*. (A) Representative immunofluorescence of Sox2 (red) and the proliferative marker Ki67 (green) in cortical sections from E13.5 *Lrig1* wild-type and *Lrig1* KO mice. VZ, ventricular zone. Scale bar: 50 µm. (B,C) Bar graphs show quantification of the total number of Sox2-positive cells per area (60,000 µm^2) (B) and the percentage of $Ki67^+$ $Sox2^+$ proliferating apical progenitor cells per area (C). Data are mean±s.e.m. from *n*=3 mice from each genotype. ***P*<0.01, two-tailed Student's *t*-test. (D) Bar graph showing $Sox2^+$ layer thickness at the dorsal, lateral and ventral regions of cortical sections from E13.5 *Lrig1* wild-type and *Lrig1* KO mice. For thickness determinations, the embryonic neocortex was divided into thirds, dorsal, lateral and ventral areas, as indicated. The ventral area begins at the top of the ganglionic eminence. The measurements were made in the middle of the indicated areas. In each case the values are relative to the total cortical thickness (VZ-cortical plate distance). Data are mean±s.e.m. from *n*=3 mice from each genotype. **P*<0.05, two-tailed Student's *t*-test. (E) Bar graph shows quantification of the percentage of $Ki67^+$ $Sox2^-$ intermediate progenitor cells proliferating in SVZ and/or IZ. Data are mean±s.e.m. from *n*=3 mice from each genotype. ns, not significant. (F) Cortical sections from E13.5 *Lrig1* wild-type and *Lrig1* KO mice analyzed for Tbr2 immunoreactivity (red) and counterstained with DAPI. IZ, intermediate zone; VZ, ventricular zone; SVZ, subventricular zone; CP, cortical plate. Scale bar: 50 µm. (F′,F″) High magnification images taken from *Lrig1* wild-type and *Lrig1* KO sections as outlined in F. CP indicates cortical plate. Scale bar: 50 µm. (G) Bar graph shows quantification of the total number of Tbr2-positive cells per area (30,000 µm^2). Data are mean±s.e.m. from *n*=3 mice from each genotype. **P*<0.05, two-tailed Student's *t*-test.

Development (2024) 151, dev202879. doi:10.1242/dev.202879

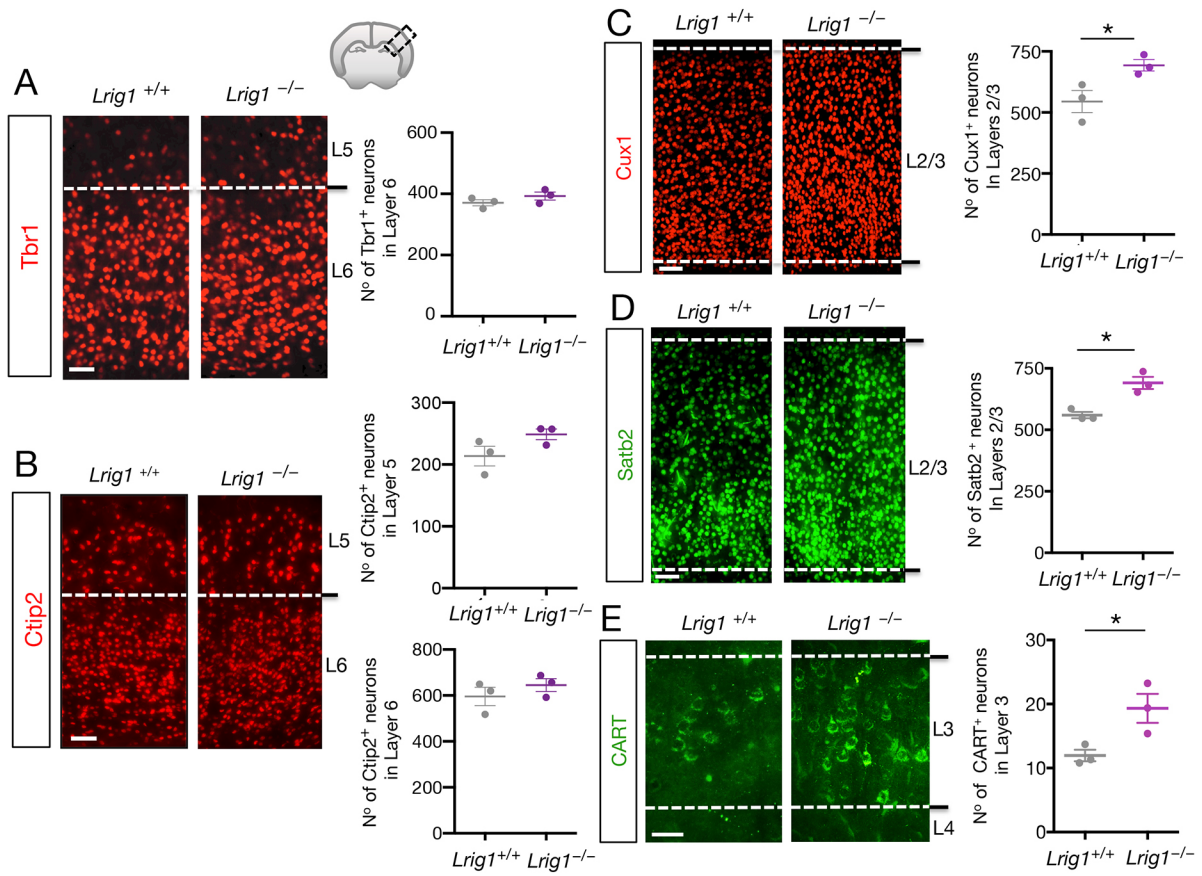

Fig. 8. Lrig1 regulates cell-fate specification of upper-layer cortical neurons. (A-E) Immunostaining of coronal sections of somatosensorial cortex from P15 mice with different lower (L5/6 or L6) and upper (L2/3 or L3) layer markers, such as Tbr1 (A), Ctip2 (B), Cux1 (C), Satb2 (D) and CART (E). Scale bars: 50 µm. Bar graphs showing the number of Tbr1$^+$ (A), Ctip2$^+$ (B), Cux1$^+$ (C), Satb2$^+$ (D) and CART$^+$ (E) glutamatergic neurons per area (100,000 µm^2) of somatosensorial (SS) cortex from P15 *Lrig1* wild-type and *Lrig1*-deficient mice are also shown for each marker. Data are mean±s.e.m., n=3 mice for each genotype. A total of six cortical sections were measured per mouse. *P<0.05, two-tailed Student's t-test. Fig. S7 shows the density measurements of Cux1, Satb2, Ctip2 and Tbr1 glutamatergic markers across all cortical layers. These markers were quantified in other layers besides those upper and lower layers shown in this figure using the same set of images.

glutamatergic neurons have already arrived at their final cortical position and the laminar organization of the neocortex is completed (Kast and Levitt, 2019). Analysis of the wild-type and knockout cortices did not show differences in either the density of layer 6 neurons stained with Tbr1 or the density of deep layer 5 and 6 (L5 and L6) neurons stained with the marker Ctip2 (Fig. 8A,B). However, knockout cortices showed a significant increase in the densities of upper-layer glutamatergic neurons positive for the markers Cux1, Satb2 and CART (Fig. 8C-E). No changes were observed in the distribution of these markers in other cortical layers (Fig. S7). Comparative analysis of the cortices of wild-type and knockout mice showed no differences in the thickness of any of the cortical layers stained with these specific markers (Fig. S8). Thus, these results demonstrate that Lrig1 selectively control the number of upper-layer glutamatergic neurons, without altering the number of deep cortical layer neurons. Together, our findings suggest that this increased production of upper-layer glutamatergic neurons could be caused by the expansion of CPs observed in *Lrig1* knockout mice at mid-embryonic stages of cortical development.

A previous study reported that Lrig1 contributes to astrocyte morphology in the postnatal cortex (Xie et al., 2022). Because of this, we also decided to evaluate whether *Lrig1* deficiency could affect astrocyte levels at the postnatal cerebral cortex using the astrocytic marker Sox9 (Sun et al., 2017). As we show in Fig. S9, we were not able to detect significant differences in the number of astrocytes placed in the neocortex upon Lrig1 elimination. Thus, in agreement with the decreased expression of Lrig1 during the cortical gliogenic period, our findings indicate that Lrig1 specifically regulates glutamatergic cortical neurogenesis without affecting astrocyte levels at postnatal day P15 of cortical development.

DISCUSSION

How neural stem and/or progenitor cells balance proliferation and self-renewal with differentiation is a crucial question relevant for our understanding of the neurodevelopmental diseases that result in the generation of incorrect numbers of neuronal or glial cells. In this study, we found that Lrig1 regulates cortical neurogenesis by controlling the cycling activity of a group of embryonic progenitors temporally specified to produce upper-layer glutamatergic neurons (Fig. 9). Here, we also show that Lrig1, a negative regulator of stem cell proliferation in different tissues, is expressed in neural stem and/or progenitor cells at early-to-mid stages of embryonic cortical development. Moreover, we show that *Lrig1* ablation promotes the expansion and proliferation of Sox2-positive radial and/or apical progenitors and increases the pool size of Tbr2-positive intermediate progenitors at embryonic stages of cortical development. In relation to this, we observed that the loss of *Lrig1* increases the expression of

Development (2024) 151, dev202879. doi:10.1242/dev.202879

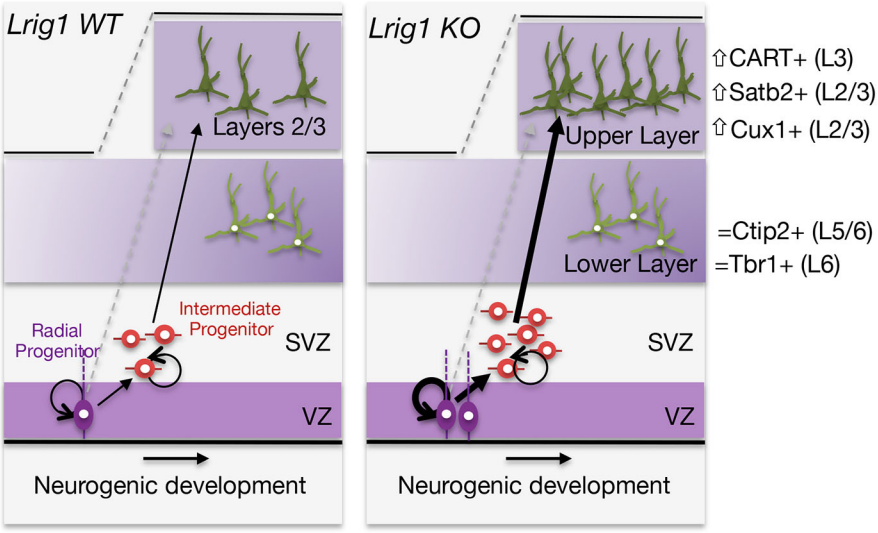

Fig. 9. Model summarizing the role of Lrig1 as a physiological regulator of glutamatergic cortical development. Lrig1 is expressed in cortical progenitors, and its ablation causes expansion and increases proliferation of radial and/or apical progenitors, which results in an increase in the population of neurogenic transit-amplifying intermediate progenitors at early-to-mid embryonic stages of cortical development. The long-lasting effect of *Lrig1* deficiency is to promote the production of upper layer glutamatergic neurons.

cyclins and other cell-cycle regulators in FGF2-induced neurospheres, thereby promoting the continued cycling of CPs rather than their exit from the cell cycle and differentiation.

Previous findings established that increased numbers of cortical excitatory neurons and excessive embryonic neurogenesis could contribute to the etiology of autism (Bruining et al., 2020; Courchesne et al., 2011; Fame et al., 2011; Lee et al., 2017; Vaccarino et al., 2009; Wegiel et al., 2010). Indeed, overproduction of excitatory upper-layer neurons in the neocortex, leading to an excitatory/inhibitory synaptic imbalance, has been associated with autism-like behaviors (Fang et al., 2014). Previously, we showed that *Lrig1*-deficient mice exhibit deficits in social interaction behavior (Alsina et al., 2016). Thus, it will be of interest to further explore whether the increased density of upper layer neurons observed here in the neocortex of *Lrig1*-deficient mice results in an excitatory/inhibitory synaptic imbalance associated with autism-related behaviors.

Lrig1 as a regulator of stem cell proliferation

Lrig1 has been involved in the control of cell proliferation of many cell types by negatively regulating mitogenic signals such as EGFR. Moreover, it has been suggested that it might also control quiescence by promoting BMP signaling (Herdenberg and Hedman, 2023; Herdenberg et al., 2021). Therefore, Lrig1 has been described as a stem cell marker in the intestine and the skin (Page et al., 2013; Powell et al., 2012), as well as a regulator of cultured skin stem cell quiescence (Jensen and Watt, 2006). In recent years, Lrig1 has been shown to be a relevant regulator of adult neural stem cell (NSC) proliferation and a genetic determinant of the adult NSC pool (Nam and Capecchi, 2020). In this study, Lrig1 is shown to be expressed in neurogenic stem cells located in the VZ and SVZ of the lateral ventricle, which generate olfactory bulb interneurons throughout adult life. In addition, we found that Lrig1 is functionally important to VZ and SVZ neurogenesis given that *Lrig1* knockout mice have increased proliferation of the cells that reside there during adulthood. Consistent with these observations, Marqués-Torrejón and collaborators have found that Lrig1 is expressed in a subset of adult NSCs from the SVZ, and that ablation of *Lrig1* in these cells results in their hyperproliferation, whereas overexpression of Lrig1 in NSCs triggered cell cycle exit (Marques-Torrejon et al., 2021).

In the present work, we tested the hypothesis that Lrig1 is relevant for the control of embryonic CP proliferation during early-to-mid stages of embryonic corticogenesis. We found that Lrig1 is expressed in radial progenitor cells at E13.5 days of cortical development. Moreover, Lrig1 ablation promotes the expansion and proliferation of Sox2-positive radial and apical progenitors, and increases the pool size of Tbr2-positive intermediate progenitors at embryonic stages of cortical development.

The role of Lrig1 at perinatal stages of corticogenesis has been studied by Jeong et al., who found that Lrig1 negatively regulates proliferation of neural stem cells by negatively modulating EGFR activity at late embryonic and perinatal stages of corticogenesis (Jeong et al., 2020), when the neurogenic to gliogenic switch takes place (Fu et al., 2021; Mukhtar and Taylor, 2018; Ohtsuka and Kageyama, 2019). In the present study, we describe a previously unreported mechanism through which Lrig1 negatively regulates FGF-driven, but not EGF-induced, neurosphere formation and cortical progenitor cell proliferation by modulating the Jak2/Stat3 pathway at early-to-mid embryonic stages, when EGFR is undetectable.

Moreover, the fact that Jak2 inhibition blocks the increased proliferation observed in *Lrig1*-deficient progenitors of E13.5 also suggest that this regulation occurs through an EGF-independent mechanism, as it has been described that activation of Stat3 by EGF requires intrinsic EGFR/Src kinase activity, but not Jak2 (Chen et al., 2011; Ma et al., 2020; Wendt et al., 2014).

Negative regulation of Jak2/Stat3 activation by Lrig1

How does Lrig1 control cortical progenitor cell proliferation at embryonic stages of cortical development? Although Lrig1 restricts the formation of neurospheres in response to FGF, intriguingly, we have not been able to detect co-immunoprecipitation between Lrig1 and FGFR1 in cell extracts prepared from embryonic cerebral cortex. However, it has been established that indirect activation of Jak2/Stat3 by FGF2 is required for the maintenance of mouse embryonic neocortical stem/progenitor cells. Conditional deletion of *Stat3* in neural progenitors reduces their capacity to form neurospheres *in vitro* in response to FGF2 (Yoshimatsu et al., 2006). Importantly, we observed by RT-PCR that *Lrig1* displays developmental expression patterns similar to those reported for *Stat3* during the embryonic development of the neocortex (Hong and Song, 2015). Furthermore, we observed co-expression of Lrig1 and Stat3 in embryonic cortical apical progenitors by immunofluorescence (Fig. S3). Interestingly, similarities between the roles played by Stat3 and Lrig1 during embryonic development of the neocortex have been reported. For example, Stat3 is expressed in embryonic radial progenitors, and its

Development (2024) 151, dev202879. doi:10.1242/dev.202879

elevated activity drives their symmetric division. For this reason, Stat3 is a major determinant of the generation and maintenance of RGCs. Finally, Stat3 controls the production of neurons that constitute the upper cortical layers without affecting the early-born neurons. Thus, like Lrig1, the contribution of Stat3 to cortical neurogenesis is also layer specific (Hong and Song, 2015). In line with this evidence, we observed that FGF2-induced neurospheres overexpressing *Lrig1* showed a reduced in the proportion of pStat3^{+} nestin^{+} progenitors compared with control spheres. Conversely, tissue extracts of neocortex prepared from E13.5 *Lrig1*-deficient mice presented a significant increase in the levels of pStat3 compared with wild-type animals. Moreover, our data show that Lrig1 dampens CP proliferation by inhibiting the activation of Jak2 induced by FGF2 (Fig. 5A-C). Hence, our findings suggest that Lrig1 could inhibit neural progenitor cell proliferation by acting as a negative regulator of upstream activators of the Jak2/Stat3 signaling pathway. As it has been described that FGF2 induces the expression of interleukin 6 (IL6) and its receptors (Bohrer et al., 2014; Todd et al., 2016), which could contribute, through an autocrine/paracrine mechanism, to activation of Jak2/Stat3-dependent proliferation of CP cells, we analyzed the role of Lrig1 as a modulator of IL6 signaling. Our findings indicate that FGF2 treatment of CPs promotes a significant increase in the expression of IL6 receptor mRNAs. Moreover, our findings demonstrate that Lrig1 regulates Stat3 activity in neurospheres treated with IL6.

Interestingly, our results are in line with previous work suggesting that Lrig1 and Stat3 might be functionally related to each other, as both *Lrig1* KO mice and transgenic animals overexpressing a constitutively active form of Stat3 in keratinocytes develop skin lesions that closely resemble psoriasis (Sano et al., 2005; Suzuki et al., 2002). Our finding showing that Lrig1 inhibits pStat3 is in agreement with these previous studies and with other work showing that Lrig1 negatively regulates the Stat3-dependent inflammatory pathway to maintain corneal homeostasis (Nakamura et al., 2014). Notably, by using a *Stat3* luciferase reporter assay, these authors showed elevated responsiveness to IL6 upon loss of *Lrig1* in mouse conjunctival fibroblasts and keratinocytes (Nakamura et al., 2014). More recently, it has also been reported that microRNA-dependent downregulation of Lrig1 promotes the survival of leukemia stem cells by activating the Stat3 pathway (Chen et al., 2021). Thus, all this evidence shows that inhibition of Stat3 activation by Lrig1 contributes to maintaining tissue homeostasis and controlling biological processes such as survival and proliferation. Although the exact molecular mechanism through which Lrig1 regulates Stat3 signaling is still unknown, previous evidence suggests that Lrig1 could control IL6 receptor signaling by acting at the level of cytokine binding, regulating IL6 receptor trafficking and/or degradation. For this reason, further analysis will be required to understand the mechanism by which Lrig1 regulates the IL6/Jak2/Stat3 signaling pathway in our system and in other biological systems.

Role of Lrig1 and Stat3 in cortical progenitors generating upper-layer neurons

Finally, a question that arises from our results is how the control of IL6/Stat3 proliferative signaling by Lrig1 regulates cell fate specification of upper-layer glutamatergic neurons. A detailed spatio-temporal analysis of Stat3 expression and activity during embryonic cortical development establishes that Stat3 activity influences proliferation and maintenance of a specific pool of Sox2-positive progenitors (Hong and Song, 2015). This study also demonstrates that Stat3 is expressed in RGCs at early-to-mid neurogenesis and is enriched in symmetrically dividing apical RGCs mainly destined to become upper-layer neurons. Moreover, the production of deep-layer neurons was normal in *Stat3* mutant mice, supporting the idea that Stat3 acts selectively on the actively dividing RG cells that produce upper-layer neurons (Hong and Song, 2015).

Interestingly, all this evidence is in agreement with the role described here for *Lrig1* mutant mice during cortical development. Thus, our results suggest that the increased production of upper-layer neurons observed in *Lrig1* KO mice could be due to the higher activity of Stat3 involved in the proliferation and maintenance of a subset of progenitors developmentally specified to produce upper-layer neurons.

Together, our results provide new insights into the role of Lrig1 as a homeostatic regulator of glutamatergic cortical neurogenesis. Additionally, our findings support a model in which Lrig1 regulates cortical neurogenesis by controlling FGF-driven IL6/Jak2/Stat3 proliferative signaling in cortical progenitors that are developmentally specified to give rise upper-layer projecting neurons.

MATERIALS AND METHODS

Lrig1 mutant mice

The *Lrig1* mutant mice have been previously described (Alsina et al., 2016; Mao et al., 2018). The colony was maintained in heterozygosis and the tested mice were littermate progeny of matings between heterozygous *Lrig* knockout mice. Animal experiments were carried out in accordance with the institutional animal care and ethics committee of the School of Medicine (CICUAL-UBA). Ethical permit number: 4094/2019.

RT-PCR and qRT-PCR

The expression of *Lrig1*, *Fgfr1*, *Egfr* and TATA box-binding protein (*Tbp*) mRNAs was analyzed by semi-quantitative RT-PCR from embryonic cortex at different developmental stages. Additionally, the ontogenic expression of *Lrig1* and *Tbp* mRNAs was measured by qRT-PCR from these embryonic cortical samples. The expression of *Ccnd1* (cyclin D1), *Ccne1* (cyclin E), *Cdkn1b* (p27), *Myc*, *Stat3*, *Il6*, *Il6st* (*Gp130*), *Il6ra* and *Tbp* mRNAs were analyzed by semi-quantitative PCR from total RNA isolated from neurospheres prepared from wild-type and *Lrig1* knockout mice, and from cortical progenitors grown in the presence of FGF2. In all cases, RNA was isolated using RNA-easy columns (Qiagen). cDNA was synthesized using multiscribe reverse transcriptase and random hexamers (Applied Biosystems). The cDNA was amplified using the following primer sets: *Tbp*, forward 5′-GGGGAGCTGTGATGTGAAGT-3′ and reverse 5′-CCAGGAAATAATTCTGGCTCA-3′; *Lrig1*, forward 5′-CTGCGTGTAAGGGAACTCAAC-3′ and reverse 5′-GATAGACCATCAAACGCTCCA-3′; *Fgfr1*, forward 5′-AGAAAGAGACAGACAACACCAAA-3′ and reverse 5′-GAATTCCTTGCCGTTTTTCA-3′; *Egfr*, forward 5′-AAATGCAACATCCTGGAGGGGGAA-3′ and reverse 5′-AGGTGGCAGACATTATTGGCA TC-3′; *Ccnd1*, forward 5′-TGCAAATGGAACTGCTTCTG-3′ and reverse 5′-CTGGCATTTTGGAGAGGAAG-3′; *Ccne1*, forward 5′-CCTCCAAAGTTGCACCAGTT-3′ and reverse 5′-CCACTTAAGGGCCTTCATCA-3′; *Cdkn1b*, forward 5′-GCGACCTGCGGCAGAAGATTC-3′ and reverse 5′-CTCCACAGTGCCAGCATTCG-3′; *Myc*, forward 5′-CCAGATCCCTGAATTGGAAA-3′ and reverse 5′-TCGTCTGCTTGAATGGACAG-3′; *Stat3*, forward 5′-GAAAAGGACATCAGTGGCAAG-3′ and reverse 5′-ACCAGGATGTTGGTCGCATC-3′; *Il6*, forward 5′- CAAAGCCAGAGTCCTTCAGAG-3′ and reverse 5′-GTCCTTAGCCACTCCTTCTG-3′; *Il6ra*, forward 5′-CCACGAGGATCAGTACGAAAG-3′ and reverse 5′-TCGTCTTGCTTTCCTTCTCAG-3′; and *Il6st*, forward 5′-GTACCTCAAACAAGCCGCTCCT-3′ and reverse 5′-TGTGAGAAGAATCCACATGCAC-3′.

Real-time PCR was performed using the SYBR Green qPCR SuperMix (Invitrogen) in an ABI7500 Sequence Detection System (Applied Biosystems), according to the manufacturer's instructions. For semi-quantitative PCR, gel bands were quantified using Gel-Pro Analyzer software.

Cell transfection and recombinant proteins

HEK293 T (from American type culture collection, ATCC) is an immortalized cell line derived from human embryonic kidney. This cell line was grown in Dulbecco's modified Eagle's medium (DMEM) with high

Development (2024) 151, dev202879. doi:10.1242/dev.202879

glucose (Invitrogen), supplemented with 10% fetal bovine serum (Invitrogen). MN1 is an immortalized mouse-derived motor neuron cell line that was cultured in DMEM supplemented with 7.5% FBS and HEPES (10 mM, Invitrogen) as previously described (De Vincenti et al., 2021; Salazar-Grueso et al., 1991). Recombinant FGF2 and EGF were obtained from R&D Systems and IL6 was purchased from Preprotech.

Primary cultures of cortical progenitors and paired cell assay

Cortical progenitors were cultured as previously described (Bonafina et al., 2018). Precursors were isolated from E14.5 rats and E13.5 mice. Cortices were mechanically dissociated and cells were plated at a density of 80,000 cells per well of 24-well plated in glass coverslips coated with Poly-D-lysine (10 µ/ml, from Sigma) in Neurobasal medium supplemented with 2% B27 (Invitrogen), 2 mM glutamine (Glutamax, from Gibco), penicillin/streptomycin (1.2 U/mi, from Sigma) and FGF2.

For paired cell assays, dissociated progenitor cells were plated at low density (~1000 cells/ml) in cortical progenitor cell media on dishes coated with Poly-D-lysine (Sigma). After 20 h, cells were fixed in 4% paraformaldehyde (PFA) and immunostained for Ki67 and with DAPI. Cell pairs were scored as symmetric proliferative division if both daughter nuclei were $Ki67^+$, as symmetric differentiative division if both were $Ki67^-$, and as asymmetric division if one nucleus was $Ki67^+$ and the other was $Ki67^-$.

Neurosphere assays

For neurosphere assays, dissociated cortical progenitor cells were seeded in 24-well plates at densities of 30,000-60,000 cells/well in 500 µl of DMEM:F12 (Invitrogen) supplemented with 2% B27 (Invitrogen), 2 mM glutamine (Glutamax, Gibco), 5 mM Hepes (Gibco), penicillin/streptomycin (1.2 U/ml, Sigma) and FGF2 (10-15 ng/ml), EGF (10 ng/ml) (R&D Systems) or IL6 (100 ng/ml) (Preprotech), as indicated in each figure legend. Cultures were allowed to grow in suspension for 5-7 days. For self-renewal analysis, primary neurospheres of ~100 µm of diameter were dissociated, passaged at a cell density of 50 cell/µl and maintained in the presence of 10-15 ng/ml of FGF2 in DMEM:F12 medium supplemented with 2% B27, 2 mM glutamine, Hepes and antibiotics. The percentage of proliferating precursors was determined as a percentage of $KI67^+$/DAPI cells and the percentage of proliferating apical precursors as percentage of $KI67^+$ $nestin^+$/total nestin cells.

Pharmacological inhibition of JAK2 kinase activity was carried out on neurospheres grown for 5 days in the presence of FGF2 (10 ng/ml). Once formed, the spheres were treated or not treated with the Jak2 inhibitor AG490 (20 µM; Sigma-Aldrich) for an additional 24 h, and then fixed at DIV6 with 4% PFA.

Retrovirus production

A replication-deficient retroviral vector based on the Moloney murine leukemia virus was used to specifically transduce cortical stem and progenitor cells. Retroviral particles were assembled using three separate plasmids containing the capside (CMV-vsvg), viral proteins (CMV-gag/pol) and the transgenes retroviral plasmid containing GFP and mouse Lrig1-Flag retroviral vector (Cellogenetics) (Alsina et al., 2016).

Plasmids were transfected onto HEK293 T cells using polyethylenimine (PEI from Polyscience) as previously described (Ledda et al., 2008). Virus-containing supernatant was harvested 48 h after transfection and concentrated by two rounds of ultracentrifugation.

Western blotting of pStat3

Cortices were lysed at 4°C in lysis buffer containing 0.5% Triton X-100, 0.1% SDS plus protease and phosphatase inhibitors. Protein lysates were clarified by centrifugation and analyzed by immunoblotting as previously described (De Vincenti et al., 2021). The blots were scanned in a Storm 845 PhosphorImager (GE Healthcare Life Sciences). The following antibodies were used: anti-pStat3 (Tyr 705) (9135, clone 58E12, Cell Signaling, 1/1000) and anti-α-tubulin (T9026, Sigma, 1/6000).

BrdU labeling

For BrdU labeling, dissociated cortical progenitors from wild-type and *Lrig1*-deficient mice were cultured in the presence of FGF2 (10 ng/ml) for 5 DIV. After this, the cells were pulse labeled with BrdU (10 µM, from Sigma) for 4 h and maintained additionally for 24 h before fixation. Cells were pretreated with 1 N HCl for 40 min at room temperature, followed by neutralization in 0.1 M borate buffer (pH 8.5) for 30 min and blocked with 10% normal donkey serum for 1 h at room temperature, after which immunostaining was performed using a mouse anti-BrdU antibody (Millipore, MAB3424, 1/300) and rabbit anti-Ki67 antibody (Abcam, AB15580, 1/600).

Immunofluorescence and microscopy

Primary cortical progenitor cells or neurospheres were washed, fixed with 4% paraformaldehyde (PFA) in PBS, permeabilized with 0.3% Triton X-100, blocked with 10% normal donkey serum (Jackson ImmunoResearch) in PBS and then incubated overnight at 4°C with primary antibodies.

Rat and mouse brains were isolated from animals fixed with 4% PFA for 4 h, maintained in 30% sucrose in PBS overnight and then embedded in OCT (Tissue-Tek) and sectioned at 25 µm. Cryostat sections were permeabilized with 0.1% Triton X-100, blocked with 10% normal donkey serum and incubated overnight at 4°C with primary antibodies.

P15 mice of selected genotypes were euthanized, perfused transcardially with 4% paraformaldehyde (PFA) in PBS under deep anesthesia. The brains were dissected and post-fixed overnight. Serial cryosections (50 µm) were made using a Leica CM1850 cryostat and processed for immunofluorescence.

The following antibodies and dilutions were used for immunofluorescence: goat polyclonal anti-Lrig1 (R&D Systems, AF3688, 1/500) (Alsina et al., 2016), rabbit polyclonal anti-Lrig1 extracellular domain was a gift from Dr Satoshi Itami (University of Osaka, Osaka, Japan; 1/1000) (De Vincenti et al., 2021; Suzuki et al., 2002), anti-nestin (Millipore, MAB353, 1/200), anti-KI67 (Abcam, ab15580, 1/500), anti-NeuN (Millipore, MAB377, 1/600), anti-Tbr1 (Abcam, ab31940, 1/600), anti-Tbr2 (Abcam, ab23345, 1/200); anti-Sox2 (SCBT, sc-17320, 1/500), anti-Pax6 (Biolegend, PRB-278P, 1/500), anti-CART (R&D Systems, AF163, 1/100), anti-Cux1 (Millipore, ABE217, 1/300), anti-Ctip2 (Abcam, ab18465, 1/600), anti-Satb2 (Abcam, ab51502, 1/300), anti Sox9 (R&D Systems, AF3075, 1/500), anti-BrdU (Millipore, MAB3424, 1/300), anti-Stat3 (Abcam, ab119352, 1/200) and anti-gp130 (SCBT, E-8 sc-376280, 1/50).

The nuclear marker DAPI (1/10,000, Sigma) was used to stain cells in culture and tissue sections. The secondary antibodies were from Jackson ImmunoResearch. Images were acquired using an Olympus IX81, an Olympus IX83 DSU confocal microscope and a LSM 880 with Ayrscan, using identical settings between control and experimental images.

For neurosphere assays (number and size), images were obtained using an Olympus IX-81 inverted microscope. For colocalization using specific markers, images of neurospheres derived from wild-type and deficient mice were obtained using an Olympus IX83 DSU confocal microscope (40× objective). Each image corresponds to an 8 µm merged stack composed of optical sections of 1 µm each. Images from neurospheres grown in the presence of retroviral particles were obtained using an LSM 880 with Ayrscan. Images were acquired by taking *z* stacks including five to eight optical slices at 1.5 µm intervals.

For embryonic tissue colocalization and quantification assays, images were obtained using an Olympus IX83 DSU confocal microscope, using a 60× or 20× objective with no saturation, no bleed through and minimized noise at a resolution of 2048×2048 pixels (16 bit). Each image corresponds to 12 or 9 µm merged stack composed of optical sections of 1 µm each.

For quantification of number and thickness of postnatal cortical layers, images were obtained using an Olympus IX83 DSU 20× objective. Each image corresponds to a merge of 16 optical sections of 1.5 µm each. All image analysis was carried out using ImageJ software.

Statistical analysis

Data are reported as mean±s.e.m., and significance was accepted at $P<0.05$. The number of independent experiments or the number of mice used in each experimental condition are described in figure legends. No statistical method was used to predetermine sample sizes, but our sample sizes are similar to those generally used in the field. For animal studies, the handling of the data was performed blind. Statistical analyses were performed in GraphPad Prism 8.0. The normal distribution of the data was evaluated with

the Shapiro–Wilk test or the Kolmogorov–Smirnov test. Normality was assumed for only small datasets . In each case, a two-tailed Student's *t*-test or one-way ANOVA analysis followed by a respective post-hoc test is indicated in figure legends.

Acknowledgements
We thank Dr Alejandro Schinder and Ignacio Satorre for technical assistance with the preparation and isolation of retroviral particles; María Mercedes Olivera, Marianela Ceol and Andrea Pecile for animal care; Lic. Nerina Villalba for confocal microscopy assistance; and UBATEC for research grant administration.

Competing interests
The authors declare no competing or financial interests.

Author contributions
Conceptualization: A.P.D.V., A.B., F.L., G.P.; Methodology: A.P.D.V., A.B.; Formal analysis: A.P.D.V., A.B., F.L., G.P.; Investigation: A.P.D.V., A.B.; Writing - original draft: G.P.; Supervision: F.L., G.P.; Funding acquisition: F.L., G.P.

Funding
This work was supported by the Agencia Nacional de Promoción Científica y Tecnológica (PICT2019-1472, PICT2019-4597 and PICT2020-1524) and the Consejo Nacional de Investigaciones Científicas y Técnicas (IBCN-P-UE 2018-22920180100009). G.P. and F.L. were supported by an Independent Career Position from the Consejo Nacional de Investigaciones Científicas y Técnicas. A.P.D.V. was supported by fellowships from the Consejo Nacional de Investigaciones Científicas y Técnicas and the Agencia Nacional de Promoción Científica y Tecnológica, and A.B. was supported by a fellowship from the Agencia Nacional de Promoción Científica y Tecnológica.

Data availability
All relevant data can be found within the article and its supplementary information.

Peer review history
The peer review history is available online at https://journals.biologists.com/dev/lookup/doi/10.1242/dev.202879.reviewer-comments.pdf

References

Ahmad, S. T., Rogers, A. D., Chen, M. J., Dixit, R., Adnani, L., Frankiw, L. S., Lawn, S. O., Blough, M. D., Alshehri, M., Wu, W. et al. (2019). Capicua regulates neural stem cell proliferation and lineage specification through control of Ets factors. *Nat. Commun.* **10**, 2000. doi:10.1038/s41467-019-09949-6

Alsina, F. C., Hita, F. J., Fontanet, P. A., Irala, D., Hedman, H., Ledda, F. and Paratcha, G. (2016). Lrig1 is a cell-intrinsic modulator of hippocampal dendrite complexity and BDNF signaling. *EMBO Rep.* **17**, 601-616. doi:10.15252/embr.201541218

Andoh, A., Bamba, S., Fujino, S., Inatomi, O., Zhang, Z., Kim, S., Takayanagi, A., Shimizu, N. and Fujiyama, Y. (2004). Fibroblast growth factor-2 stimulates interleukin-6 secretion in human pancreatic periacinar myofibroblasts. *Pancreas* **29**, 278-283. doi:10.1097/00006676-200411000-00006

Bohrer, L. R., Chuntova, P., Bade, L. K., Beadnell, T. C., Leon, R. P., Brady, N. J., Ryu, Y., Goldberg, J. E., Schmechel, S. C., Koopmeiners, J. S. et al. (2014). Activation of the FGFR-STAT3 pathway in breast cancer cells induces a hyaluronan-rich microenvironment that licenses tumor formation. *Cancer Res.* **74**, 374-386. doi:10.1158/0008-5472.CAN-13-2469

Bonafina, A., Fontanet, P. A., Paratcha, G. and Ledda, F. (2018). GDNF/GFRalpha1 complex abrogates self-renewing activity of cortical neural precursors inducing their differentiation. *Stem Cell Rep.* **10**, 1000-1015. doi:10.1016/j.stemcr.2018.01.019

Bonnefont, J. and Vanderhaeghen, P. (2021). Neuronal fate acquisition and specification: time for a change. *Curr. Opin. Neurobiol.* **66**, 195-204. doi:10.1016/j.conb.2020.12.006

Borrell, V. and Reillo, I. (2012). Emerging roles of neural stem cells in cerebral cortex development and evolution. *Dev. Neurobiol.* **72**, 955-971. doi:10.1002/dneu.22013

Bruining, H., Hardstone, R., Juarez-Martinez, E. L., Sprengers, J., Avramiea, A. E., Simpraga, S., Houtman, S. J., Poil, S. S., Dallares, E., Palva, S. et al. (2020). Measurement of excitation-inhibition ratio in autism spectrum disorder using critical brain dynamics. *Sci. Rep.* **10**, 9195. doi:10.1038/s41598-020-65500-4

Burrows, R. C., Wancio, D., Levitt, P. and Lillien, L. (1997). Response diversity and the timing of progenitor cell maturation are regulated by developmental changes in EGFR expression in the cortex. *Neuron* **19**, 251-267. doi:10.1016/S0896-6273(00)80937-X

Chen, J.-X., Xu, L.-L., Wang, X.-C., Qin, H.-Y. and Wang, J.-L. (2011). Involvement of c-Src/STAT3 signal in EGF-induced proliferation of rat spermatogonial stem cells. *Mol. Cell. Biochem.* **358**, 67-73. doi:10.1007/s11010-011-0922-2

Chen, L., Guo, Z., Zhou, Y., Ni, J., Zhu, J., Fan, X., Chen, X., Liu, Y., Li, Z. and Zhou, H. (2021). microRNA-1246-containing extracellular vesicles from acute myeloid leukemia cells promote the survival of leukemia stem cells via the LRIG1-meditated STAT3 pathway. *Aging (Albany NY)* **13**, 13644-13662. doi:10.18632/aging.202893

Courchesne, E., Mouton, P. R., Calhoun, M. E., Semendeferi, K., Ahrens-Barbeau, C., Hallet, M. J., Barnes, C. C. and Pierce, K. (2011). Neuron number and size in prefrontal cortex of children with autism. *JAMA* **306**, 2001-2010. doi:10.1001/jama.2011.1638

De Vincenti, A. P., Alsina, F. C., Ferrero Restelli, F., Hedman, H., Ledda, F. and Paratcha, G. (2021). Lrig1 and Lrig3 cooperate to control Ret receptor signaling, sensory axonal growth and epidermal innervation. *Development* **148**, dev197020. doi:10.1242/dev.197020

Dehay, C. and Kennedy, H. (2007). Cell-cycle control and cortical development. *Nat. Rev. Neurosci.* **8**, 438-450. doi:10.1038/nrn2097

Di Bella, D. J., Habibi, E., Stickels, R. R., Scalia, G., Brown, J., Yadollahpour, P., Yang, S. M., Abbate, C., Biancalani, T., Macosko, E. Z. et al. (2021). Molecular logic of cellular diversification in the mouse cerebral cortex. *Nature* **595**, 554-559. doi:10.1038/s41586-021-03670-5

Dwyer, N. D., Chen, B., Chou, S. J., Hippenmeyer, S., Nguyen, L. and Ghashghaei, H. T. (2016). Neural stem cells to cerebral cortex: emerging mechanisms regulating progenitor behavior and productivity. *J. Neurosci.* **36**, 11394-11401. doi:10.1523/JNEUROSCI.2359-16.2016

Englund, C., Fink, A., Lau, C., Pham, D., Daza, R. A., Bulfone, A., Kowalczyk, T. and Hevner, R. F. (2005). Pax6, Tbr2, and Tbr1 are expressed sequentially by radial glia, intermediate progenitor cells, and postmitotic neurons in developing neocortex. *J. Neurosci.* **25**, 247-251. doi:10.1523/JNEUROSCI.2899-04.2005

Fame, R. M., Macdonald, J. L. and Macklis, J. D. (2011). Development, specification, and diversity of callosal projection neurons. *Trends Neurosci.* **34**, 41-50. doi:10.1016/j.tins.2010.10.002

Fang, W. Q., Chen, W. W., Jiang, L., Liu, K., Yung, W. H., Fu, A. K. Y. and Ip, N. Y. (2014). Overproduction of upper-layer neurons in the neocortex leads to autism-like features in mice. *Cell Rep.* **9**, 1635-1643. doi:10.1016/j.celrep.2014.11.003

Fox, I. J. and Kornblum, H. I. (2005). Developmental profile of ErbB receptors in murine central nervous system: implications for functional interactions. *J. Neurosci. Res.* **79**, 584-597. doi:10.1002/jnr.20381

Fu, Y., Yang, M., Yu, H., Wang, Y., Wu, X., Yong, J., Mao, Y., Cui, Y., Fan, X., Wen, L. et al. (2021). Heterogeneity of glial progenitor cells during the neurogenesis-to-gliogenesis switch in the developing human cerebral cortex. *Cell Rep.* **34**, 108788. doi:10.1016/j.celrep.2021.108788

Gallagher, D., Norman, A. A., Woodard, C. L., Yang, G., Gauthier-Fisher, A., Fujitani, M., Vessey, J. P., Cancino, G. I., Sachewsky, N., Woltjen, K. et al. (2013). Transient maternal IL-6 mediates long-lasting changes in neural stem cell pools by deregulating an endogenous self-renewal pathway. *Cell Stem Cell* **13**, 564-576. doi:10.1016/j.stem.2013.10.002

Gaspard, N., Bouschet, T., Hourez, R., Dimidschstein, J., Naeije, G., Van Den Ameele, J., Espuny-Camacho, I., Herpoel, A., Passante, L., Schiffmann, S. N. et al. (2008). An intrinsic mechanism of corticogenesis from embryonic stem cells. *Nature* **455**, 351-357. doi:10.1038/nature07287

Gur, G., Rubin, C., Katz, M., Amit, I., Citri, A., Nilsson, J., Amariglio, N., Henriksson, R., Rechavi, G., Hedman, H. et al. (2004). LRIG1 restricts growth factor signaling by enhancing receptor ubiquitylation and degradation. *EMBO J.* **23**, 3270-3281. doi:10.1038/sj.emboj.7600342

Hedman, H. and Henriksson, R. (2007). LRIG inhibitors of growth factor signalling - double-edged swords in human cancer? *Eur. J. Cancer* **43**, 676-682. doi:10.1016/j.ejca.2006.10.021

Herdenberg, C. and Hedman, H. (2023). HYPOTHESIS: do LRIG proteins regulate stem cell quiescence by promoting BMP signaling? *Stem Cell Rev. Rep.* **19**, 59-66. doi:10.1007/s12015-022-10442-9

Herdenberg, C., Mutie, P. M., Billing, O., Abdullah, A., Strawbridge, R. J., Dahlman, I., Tuck, S., Holmlund, C., Arner, P., Henriksson, R. et al. (2021). LRIG proteins regulate lipid metabolism via BMP signaling and affect the risk of type 2 diabetes. *Commun. Biol.* **4**, 90. doi:10.1038/s42003-020-01613-w

Hong, S. and Song, M. R. (2015). Signal transducer and activator of transcription-3 maintains the stemness of radial glia at mid-neurogenesis. *J. Neurosci.* **35**, 1011-1023. doi:10.1523/JNEUROSCI.2119-14.2015

Jensen, K. B. and Watt, F. M. (2006). Single-cell expression profiling of human epidermal stem and transit-amplifying cells: Lrig1 is a regulator of stem cell quiescence. *Proc. Natl. Acad. Sci. USA* **103**, 11958-11963. doi:10.1073/pnas.0601886103

Jensen, K. B., Collins, C. A., Nascimento, E., Tan, D. W., Frye, M., Itami, S. and Watt, F. M. (2009). Lrig1 expression defines a distinct multipotent stem cell population in mammalian epidermis. *Cell Stem Cell* **4**, 427-439. doi:10.1016/j.stem.2009.04.014

Jeong, D., Lozano Casasbuenas, D., Gengatharan, A., Edwards, K., Saghatelyan, A., Kaplan, D. R., Miller, F. D. and Yuzwa, S. A. (2020). LRIG1-mediated inhibition of EGF receptor signaling regulates neural precursor cell proliferation in the neocortex. *Cell Rep.* **33**, 108257. doi:10.1016/j.celrep.2020.108257

Ji, Y., Kumar, R., Gokhale, A., Chao, H. P., Rycaj, K., Chen, X., Li, Q. and Tang, D. G. (2022). LRIG1, a regulator of stem cell quiescence and a pleiotropic feedback tumor suppressor. *Semin. Cancer Biol.* **82**, 120-133. doi:10.1016/j.semcancer.2020.12.016

Kam, J. W., Raja, R. and Cloutier, J. F. (2014). Cellular and molecular mechanisms regulating embryonic neurogenesis in the rodent olfactory epithelium. *Int. J. Dev. Neurosci.* **37**, 76-86. doi:10.1016/j.ijdevneu.2014.06.017

Kast, R. J. and Levitt, P. (2019). Precision in the development of neocortical architecture: from progenitors to cortical networks. *Prog. Neurobiol.* **175**, 77-95. doi:10.1016/j.pneurobio.2019.01.003

Kilpatrick, T. J. and Bartlett, P. F. (1995). Cloned multipotential precursors from the mouse cerebrum require FGF-2, whereas glial restricted precursors are stimulated with either FGF-2 or EGF. *J. Neurosci.* **15**, 3653-3661. doi:10.1523/JNEUROSCI.15-05-03653.1995

Kornblum, H. I., Hussain, R. J., Bronstein, J. M., Gall, C. M., Lee, D. C. and Seroogy, K. B. (1997). Prenatal ontogeny of the epidermal growth factor receptor and its ligand, transforming growth factor alpha, in the rat brain. *J. Comp. Neurol.* **380**, 243-261. doi:10.1002/(SICI)1096-9861(19970407)380:2<243::AID-CNE7>3.0.CO;2-3

Kozawa, O., Suzuki, A. and Uematsu, T. (1997). Basic fibroblast growth factor induces interleukin-6 synthesis in osteoblasts: autoregulation by protein kinase C. *Cell. Signal.* **9**, 463-468. doi:10.1016/S0898-6568(97)00043-0

Laederich, M. B., Funes-Duran, M., Yen, L., Ingalla, E., Wu, X., Carraway, K. L., 3rd and Sweeney, C. (2004). The leucine-rich repeat protein LRIG1 is a negative regulator of ErbB family receptor tyrosine kinases. *J. Biol. Chem.* **279**, 47050-47056. doi:10.1074/jbc.M409703200

Ledda, F. and Paratcha, G. (2016). Assembly of neuronal connectivity by neurotrophic factors and leucine-rich repeat proteins. *Front. Cell Neurosci.* **10**, 199. doi:10.3389/fncel.2016.00199

Ledda, F., Bieraugel, O., Fard, S. S., Vilar, M. and Paratcha, G. (2008). Lrig1 is an endogenous inhibitor of Ret receptor tyrosine kinase activation, downstream signaling, and biological responses to GDNF. *J. Neurosci.* **28**, 39-49. doi:10.1523/JNEUROSCI.2196-07.2008

Lee, E., Lee, J. and Kim, E. (2017). Excitation/inhibition imbalance in animal models of autism spectrum disorders. *Biol. Psychiatry* **81**, 838-847. doi:10.1016/j.biopsych.2016.05.011

Lillien, L. and Raphael, H. (2000). BMP and FGF regulate the development of EGF-responsive neural progenitor cells. *Development* **127**, 4993-5005. doi:10.1242/dev.127.22.4993

Lukaszewicz, A., Savatier, P., Cortay, V., Kennedy, H. and Dehay, C. (2002). Contrasting effects of basic fibroblast growth factor and neurotrophin 3 on cell cycle kinetics of mouse cortical stem cells. *J. Neurosci.* **22**, 6610-6622. doi:10.1523/JNEUROSCI.22-15-06610.2002

Ma, J. H., Qin, L. and Li, X. (2020). Role of STAT3 signaling pathway in breast cancer. *Cell Commun. Signal* **18**, 33. doi:10.1186/s12964-020-0527-z

Mao, F., Holmlund, C., Faraz, M., Wang, W., Bergenheim, T., Kvarnbrink, S., Johansson, M., Henriksson, R. and Hedman, H. (2018). Lrig1 is a haploinsufficient tumor suppressor gene in malignant glioma. *Oncogenesis* **7**, 13. doi:10.1038/s41389-017-0012-8

Marques-Torrejon, M. A., Williams, C. A. C., Southgate, B., Alfazema, N., Clements, M. P., Garcia-Diaz, C., Blin, C., Arranz-Emparan, N., Fraser, J., Gammoh, N. et al. (2021). LRIG1 is a gatekeeper to exit from quiescence in adult neural stem cells. *Nat. Commun.* **12**, 2594. doi:10.1038/s41467-021-22813-w

Mira, H., Andreu, Z., Suh, H., Lie, D. C., Jessberger, S., Consiglio, A., San Emeterio, J., Hortiguela, R., Marques-Torrejon, M. A., Nakashima, K. et al. (2010). Signaling through BMPR-IA regulates quiescence and long-term activity of neural stem cells in the adult hippocampus. *Cell Stem Cell* **7**, 78-89. doi:10.1016/j.stem.2010.04.016

Molyneaux, B. J., Arlotta, P., Menezes, J. R. and Macklis, J. D. (2007). Neuronal subtype specification in the cerebral cortex. *Nat. Rev. Neurosci.* **8**, 427-437. doi:10.1038/nrn2151

Mukhtar, T. and Taylor, V. (2018). Untangling cortical complexity during development. *J. Exp. Neurosci.* **12**, 117906951875933. doi:10.1177/1179069518759332

Nakamura, T., Hamuro, J., Takaishi, M., Simmons, S., Maruyama, K., Zaffalon, A., Bentley, A. J., Kawasaki, S., Nagata-Takaoka, M., Fullwood, N. J. et al. (2014). LRIG1 inhibits STAT3-dependent inflammation to maintain corneal homeostasis. *J. Clin. Invest.* **124**, 385-397. doi:10.1172/JCI71488

Nam, H. S. and Capecchi, M. R. (2020). Lrig1 expression prospectively identifies stem cells in the ventricular-subventricular zone that are neurogenic throughout adult life. *Neural Dev.* **15**, 3. doi:10.1186/s13064-020-00139-5

Nam, H. S. and Capecchi, M. R. (2023). Lrig1 expression identifies quiescent stem cells in the ventricular-subventricular zone from postnatal development to adulthood and limits their persistent hyperproliferation. *Neural Dev.* **18**, 1. doi:10.1186/s13064-022-00169-1

Neirinckx, V., Hedman, H. and Niclou, S. P. (2017). Harnessing LRIG1-mediated inhibition of receptor tyrosine kinases for cancer therapy. *Biochim. Biophys. Acta Rev. Cancer* **1868**, 109-116. doi:10.1016/j.bbcan.2017.02.007

Ohtsuka, T. and Kageyama, R. (2019). Regulation of temporal properties of neural stem cells and transition timing of neurogenesis and gliogenesis during mammalian neocortical development. *Semin. Cell Dev. Biol.* **95**, 4-11. doi:10.1016/j.semcdb.2019.01.007

Page, M. E., Lombard, P., Ng, F., Gottgens, B. and Jensen, K. B. (2013). The epidermis comprises autonomous compartments maintained by distinct stem cell populations. *Cell Stem Cell* **13**, 471-482. doi:10.1016/j.stem.2013.07.010

Powell, A. E., Wang, Y., Li, Y., Poulin, E. J., Means, A. L., Washington, M. K., Higginbotham, J. N., Juchheim, A., Prasad, N., Levy, S. E. et al. (2012). The pan-ErbB negative regulator Lrig1 is an intestinal stem cell marker that functions as a tumor suppressor. *Cell* **149**, 146-158. doi:10.1016/j.cell.2012.02.042

Reynolds, B. A. and Weiss, S. (1996). Clonal and population analyses demonstrate that an EGF-responsive mammalian embryonic CNS precursor is a stem cell. *Dev. Biol.* **175**, 1-13. doi:10.1006/dbio.1996.0090

Salazar-Grueso, E. F., Kim, S. and Kim, H. (1991). Embryonic mouse spinal cord motor neuron hybrid cells. *Neuroreport* **2**, 505-508. doi:10.1097/00001756-199109000-00002

Sano, S., Chan, K. S., Carbajal, S., Clifford, J., Peavey, M., Kiguchi, K., Itami, S., Nickoloff, B. J. and Digiovanni, J. (2005). Stat3 links activated keratinocytes and immunocytes required for development of psoriasis in a novel transgenic mouse model. *Nat. Med.* **11**, 43-49. doi:10.1038/nm1162

Sessa, A., Mao, C. A., Hadjantonakis, A. K., Klein, W. H. and Broccoli, V. (2008). Tbr2 directs conversion of radial glia into basal precursors and guides neuronal amplification by indirect neurogenesis in the developing neocortex. *Neuron* **60**, 56-69. doi:10.1016/j.neuron.2008.09.028

Shattuck, D. L., Miller, J. K., Laederich, M., Funes, M., Petersen, H., Carraway, K. L., 3rd and Sweeney, C. (2007). LRIG1 is a novel negative regulator of the Met receptor and opposes Met and Her2 synergy. *Mol. Cell. Biol.* **27**, 1934-1946. doi:10.1128/MCB.00757-06

Simion, C., Cedano-Prieto, M. E. and Sweeney, C. (2014). The LRIG family: enigmatic regulators of growth factor receptor signaling. *Endocr Relat. Cancer* **21**, R431-R443. doi:10.1530/ERC-14-0179

Sun, W., Cornwell, A., Li, J., Peng, S., Osorio, M. J., Aalling, N., Wang, S., Benraiss, A., Lou, N., Goldman, S. A. et al. (2017). SOX9 Is an Astrocyte-Specific Nuclear Marker in the Adult Brain Outside the Neurogenic Regions. *J. Neurosci.* **37**, 4493-4507. doi:10.1523/JNEUROSCI.3199-16.2017

Suzuki, Y., Miura, H., Tanemura, A., Kobayashi, K., Kondoh, G., Sano, S., Ozawa, K., Inui, S., Nakata, A., Takagi, T. et al. (2002). Targeted disruption of LIG-1 gene results in psoriasiform epidermal hyperplasia. *FEBS Lett.* **521**, 67-71. doi:10.1016/S0014-5793(02)02824-7

Telley, L., Govindan, S., Prados, J., Stevant, I., Nef, S., Dermitzakis, E., Dayer, A. and Jabaudon, D. (2016). Sequential transcriptional waves direct the differentiation of newborn neurons in the mouse neocortex. *Science* **351**, 1443-1446. doi:10.1126/science.aad8361

Todd, L., Squires, N., Suarez, L. and Fischer, A. J. (2016). Jak/Stat signaling regulates the proliferation and neurogenic potential of Muller glia-derived progenitor cells in the avian retina. *Sci. Rep.* **6**, 35703. doi:10.1038/srep35703

Toma, K. and Hanashima, C. (2015). Switching modes in corticogenesis: mechanisms of neuronal subtype transitions and integration in the cerebral cortex. *Front. Neurosci.* **9**, 274. doi:10.3389/fnins.2015.00274

Vaccarino, F. M., Grigorenko, E. L., Smith, K. M. and Stevens, H. E. (2009). Regulation of cerebral cortical size and neuron number by fibroblast growth factors: implications for autism. *J. Autism Dev. Disord.* **39**, 511-520. doi:10.1007/s10803-008-0653-8

Van Erp, S., Van Den Heuvel, D. M. A., Fujita, Y., Robinson, R. A., Hellemons, A., Adolfs, Y., Van Battum, E. Y., Blokhuis, A. M., Kuijpers, M., Demmers, J. A. A. et al. (2015). Lrig2 negatively regulates ectodomain shedding of axon guidance receptors by ADAM proteases. *Dev. Cell* **35**, 537-552. doi:10.1016/j.devcel.2015.11.008

Wang, Y., Poulin, E. J. and Coffey, R. J. (2013). LRIG1 is a triple threat: ERBB negative regulator, intestinal stem cell marker and tumour suppressor. *Br. J. Cancer* **108**, 1765-1770. doi:10.1038/bjc.2013.138

Wegiel, J., Kuchna, I., Nowicki, K., Imaki, H., Wegiel, J., Marchi, E., Ma, S. Y., Chauhan, A., Chauhan, V., Bobrowicz, T. W. et al. (2010). The neuropathology of autism: defects of neurogenesis and neuronal migration, and dysplastic changes. *Acta Neuropathol.* **119**, 755-770. doi:10.1007/s00401-010-0655-4

Wendt, M. K., Balanis, N., Carlin, C. R. and Schiemann, W. P. (2014). STAT3 and epithelial-mesenchymal transitions in carcinomas. *JAKSTAT* **3**, e28975. doi:10.4161/jkst.28975

Wong, V. W., Stange, D. E., Page, M. E., Buczacki, S., Wabik, A., Itami, S., Van De Wetering, M., Poulsom, R., Wright, N. A., Trotter, M. W. et al. (2012). Lrig1 controls intestinal stem-cell homeostasis by negative regulation of ErbB signalling. *Nat. Cell Biol.* **14**, 401-408. doi:10.1038/ncb2464

Xie, Y., Kuan, A. T., Wang, W., Herbert, Z. T., Mosto, O., Olukoya, O., Adam, M., Vu, S., Kim, M., Tran, D. et al. (2022). Astrocyte-neuron crosstalk through Hedgehog signaling mediates cortical synapse development. *Cell Rep.* **38**, 110416. doi:10.1016/j.celrep.2022.110416

Yoshimatsu, T., Kawaguchi, D., Oishi, K., Takeda, K., Akira, S., Masuyama, N. and Gotoh, Y. (2006). Non-cell-autonomous action of STAT3 in maintenance of neural precursor cells in the mouse neocortex. *Development* **133**, 2553-2563. doi:10.1242/dev.02419

Zhao, H., Tanegashima, K., Ro, H. and Dawid, I. B. (2008). Lrig3 regulates neural crest formation in Xenopus by modulating Fgf and Wnt signaling pathways. *Development* **135**, 1283-1293. doi:10.1242/dev.015073